mathematics

Article

Fixed/Preassigned-Time Synchronization of Fuzzy Memristive Fully Quaternion-Valued Neural Networks Based on Event-Triggered Control

Shichao Jia [1], Cheng Hu [1,2] and Haijun Jiang [3,*]

[1] College of Mathematics and System Sciences, Xinjiang University, Urumqi 830017, China; jiashichao@stu.xju.edu.cn (S.J.); hucheng@xju.edu.cn (C.H.)
[2] Xinjiang Key Laboratory of Applied Mathematics, Urumqi 830017, China
[3] College of Mathematics and Statistics, Yili Normal University, Yining 835000, China
* Correspondence: jianghaijunxju@163.com

Abstract: In this paper, the fixed-time and preassigned-time synchronization issues of fully quaternion-valued fuzzy memristive neural networks are studied based on the dynamic event-triggered control mechanism. Initially, the fuzzy rules are defined within the quaternion domain and the relevant properties are established through rigorous analysis. Subsequently, to conserve resources and enhance the efficiency of the controller, a kind of dynamic event-triggered control mechanism is introduced for the fuzzy memristive neural networks. Based on the non-separation analysis, fixed-time and preassigned-time synchronization criteria are presented and the Zeno phenomenon under the event-triggered mechanism is excluded successfully. Finally, the effectiveness of the theoretical results is verified through numerical simulations.

Keywords: quaternion-valued fuzzy memristive neural network; fixed-time synchronization; dynamic event-triggered control; preassigned-time synchronization; non-separation approach

MSC: 35A23; 35A01; 35B38

check for updates

Citation: Jia, S.; Hu, C.; Jiang, H. Fixed/Preassigned-Time Synchronization of Fuzzy Memristive Fully Quaternion-Valued Neural Networks Based on Event-Triggered Control. *Mathematics* **2024**, *12*, 1276. https://doi.org/10.3390/math12091276

Academic Editors: Asier Ibeas and Ivo Petráš

Received: 30 March 2024
Revised: 12 April 2024
Accepted: 22 April 2024
Published: 23 April 2024

1. Introduction

Over the past several decades, artificial neural networks have taken center stage in technology research. At present, in an attempt to mimic the complex operations of the human brain, researchers have embarked on the exploration of a novel form of artificial neural network known as the fuzzy memristive neural network (FMNN). This groundbreaking neural network blends fuzzy logic and memristor technology, boosting the deep learning prowess of neural networks by imitating the synaptic behavior inherent in the human brain. The fuzzy memristive neural network not only facilitates the storage and processing of substantial volumes of data but also enhances adaptability and efficiency in the machine learning process. This form of neural network holds immense potential for propelling the evolution of artificial intelligence and heralding a novel technological revolution. Currently, researchers in the field of FMNN have produced several excellent results [1–4]. For instance, in [1], an impulsive sampled data communication mechanism is proposed to investigate the anti-synchronization of FMNNs. Gong et al. presented the T-S FMNN synchronization criterion in [3]. Additionally, Wang et al. investigated the fixed-time and preassigned-time synchronization of FMNNs [4].

It is important to note that the aforementioned studies on FMNN have been conducted in the real number domain. As a generalization of real-valued numbers and complex-valued numbers, the algebraic structure of quaternions is well-recognized for its ability to empower networks with increased representational capacity and a reduced count of parameters when addressing complex interrelationships and patterns. By integrating quaternion-based weights and activation functions, the quaternion-valued neural network (QVNN) improves the traditional mathematical representation of neurons and makes it possible to process multi-channel data, including color imagery [5], video content [6], and 3D spatial information [7]. Currently, the dynamic properties of QVNN have been widely concerned, such as dissipativity [8,9], stability [10,11], optimization [12], and synchronization [13,14]. The fusion of QVNN, known for its efficient data representation, with the high fault tolerance characteristic of FMNN, has given rise to the innovative quaternion-valued fuzzy neural network model. This synergetic model amplifies the network's resilience to noise and data incompleteness while preserving the inherent multi-dimensional correlations present within the data.

Synchronization pertains to the coordinated process where neurons or neuron clusters within a neural network achieve a uniform or coherent state of activity via mutual influence. This phenomenon has become a significant topic in the field of QVNNs. Zhang et al. provided several criteria for synchronization of quaternion-valued memristive neural networks (QVMNNs) by designing adaptive control strategies [15]. The exponential synchronization for QVMNNs with time-varying delayed were addressed in [16,17]. Moreover, the issues of synchronization associated with quaternion-valued fuzzy neural networks have been reported in [18–20]. Nevertheless, due to the complexity of quaternion-valued and memristor-based neurons, there are fewer related references on quaternion-valued fuzzy memristive neural networks (QVFMNNs). Furthermore, the fuzzy operations introduced into the model of QVMNN, the design of controller, and the theoretical proof are not a trivial generalization. We need to design new control algorithms, use special techniques to deal with the fuzzy term, and study the synchronization of QVFMNN.

Traditional research on synchronous systems typically emphasizes exponential and asymptotic synchronization. However, these techniques frequently fail to achieve synchronization within a limited time. Consequently, there has been an increasing interest in research on fixed-time synchronization (FITS) to meet practical application requirements. FITS aims to attain consistency of states among all neurons in a network within a finite time, regardless of initial conditions. There are several outstanding results about FITS [21–24]. Tang et al. designed a continuous sampling and non-chattering controller to achieve the FITS of neural networks [21]. The FITS of memristor-based neural networks was investigated by a continuous sampling feedback control in [24]. With the development of time, more investigation in the engineering field is needed to achieve synchronization in an ideal predetermined time, in which the convergence time is independent of the system and controller parameters. Hu et al. have proposed a mature theory of prescribed-time stability [25], which successfully extended the fixed-time stability theory. Subsequently, numerous noteworthy achievements have been made [26–30]. The preassigned-time synchronization (PETS) of complex-valued memristive neural networks was studied in [29]. It is important to note that most of the aforementioned research is based on continuous time-triggered control. When it comes to resource utilization, this control wastes computing and energy resources by performing control tasks periodically. In addition, if the sampling period is relatively small, a large number of redundant sampling signals will be released into the communication network with limited bandwidth, which will inevitably cause network congestion.

Event-triggered control is an important method in the design of modern control systems, with the core concept of reducing redundant data transmission and improving computation efficiency by designing event-triggered mechanisms. In an event-triggered control framework, the update of control inputs is not performed at fixed time points, but rather depends on specific changes in the system state or the occurrence of certain events. This approach is in stark contrast to traditional periodic sampling control, which continuously checks and updates the system state at fixed time intervals, regardless of whether there is a significant change in the system state. Static event-triggered control is one of the more traditional event-triggering methods. In a static event-triggering mechanism, the triggering condition typically relies on a determined relationship between the current system state and the sampling error. When the system error exceeds a preset threshold, a control action is triggered. The design goal of this mechanism is to ensure that the system state can gradually converge to the desired target or origin [31–35]. Dynamic event-triggered control introduces internal dynamic variables to improve upon the static method. The dynamic event-triggering mechanism allows the triggering conditions to adjust dynamically with time and changes in system state, which can further save resources while maintaining or enhancing system performance. By introducing dynamic variables, the control system can adjust the event-triggering rules based on real-time system performance and predetermined stability requirements, thus increasing the interval between executions and reducing unnecessary control updates while ensuring stability and performance metrics [36–39].

Based on the preceding analysis, this study aims to address the synchronization of QVFMNNs by a kind of dynamic event-triggered control mechanism in both fixed-time and prescribed-time scenarios. The main contributions and innovations of this article can be highlighted as follows.

(1) Building on the foundational insights of established methods like the lexicographic order method and the metric function method [40–42], this paper embarks on a novel journey within the realm of quaternion analysis by redefining fuzzy rules. It further fortifies this innovation by rigorously analyzing and validating the accuracy and efficacy of the lemmas tied to the fuzzy rules, thereby setting a new benchmark in theoretical exploration.

(2) Moving beyond traditional static event-triggering control mechanisms [43,44] with an eye towards enhancing communication efficiency, this paper introduces an innovative approach through the formulation of quaternion-valued dynamic event-triggering control strategies devoid of linear components. This strategic framework is designed to guarantee both FITS and PETS within the context of QVFMNNs. Additionally, the paper adeptly eliminates the potential for Zeno phenomena within the system by employing a methodical application of the proof by contradiction.

(3) Different from the conventional separation technique, the FITS and PETS of QVFMNN are discussed through a direct analytical approach. Consequently, several flexible criteria are established for achieving FITS and PETS of QVFMNN and the upper bound of the setting time is provided explicitly.

In Section 2, the necessary preliminaries are introduced. Section 3 are dedicated to exploring the FITS and PETS of QVFMNNs through the lens of event-triggered control mechanisms, respectively. In Section 4, two numerical examples are present to substantiate the theoretical results. The paper is summarized in Section 5.

2. Model Description and Preliminaries

A quaternion-valued fuzzy memristive neural network is given by

$$
\begin{aligned}
\dot{w}_p(t) = {} & -d_p(w_p(t))w_p(t) + \sum_{q\in\mathbf{N}} a_{pq}(w_p(t))f_q(w_q(t)) + \sum_{q\in\mathbf{N}} b_{pq}(w_p(t))g_q(w_q(m_{pq}(t))) \\
& + \bigvee_{q\in\mathbf{N}} \theta_{pq}g_q(x_q(m_{pq}(t))) + \bigwedge_{q\in\mathbf{N}} \sigma_{pq}g_q(w_q(m_{pq}(t))) + \sum_{q\in\mathbf{N}} c_{pq}\eta_q \\
& + \bigvee_{q\in\mathbf{N}} \phi_{pq}\eta_q + \bigwedge_{q\in\mathbf{N}} \psi_{pq}\eta_q + \xi_p, \quad p \in \mathbf{N},
\end{aligned} \tag{1}
$$

where $w_p(t) \in \mathbb{Q}$ is the state of the pth unit, $d_p(w_p(t)) \in \mathbb{Q}$ is the feedback self-connection weight, $a_{pq}(w_p(t))$, $b_{pq}(w_p(t)) \in \mathbb{Q}$ are the connection weights, $f_q(\cdot)$ and $g_q(\cdot) : \mathbb{Q} \to \mathbb{Q}$ are quaternion-valued activation functions, $m_{pq}(t) \leq t$ is the generalized time delay, c_{pq}, ϕ_{pq}, $\psi_{pq} \in \mathbb{Q}$ mean the connection weights of fuzzy feed-forward template, η_p and ξ_p denote the bias and the external input of the pth neuron, respectively. $\bigvee$ and $\bigwedge$ denote the fuzzy operations of OR and AND, and θ_{pq} and $\sigma_{pq} \in \mathbb{Q}$ purport the connection weights of the fuzzy feedback MIN template and feed forward MAX template. In addition,

$w_p(s) = \varrho_p(s) \in C([-\digamma, 0])$ is the initial state of the network (1), in which $\digamma = \max_{p,q\in\mathbb{N}}\{|m_{pq}(0)|\}$. Moreover, the connection weights $d_p(w_p(t)), a_{pq}(w_p(t)), b_{pq}(w_p(t))$ satisfy

$$d_p(w_p(t)) = \begin{cases} \check{d}_p = \check{d}_p^R + \check{d}_p^I i + \check{d}_p^J j + \check{d}_p^K k, & |w_p(t)|_1 \le h_p, \\ \hat{d}_p = \hat{d}_p^R + \hat{d}_p^I i + \hat{d}_p^J j + \hat{d}_p^K k, & |w_p(t)|_1 > h_p, \end{cases}$$

$$a_{pq}(w_p(t)) = \begin{cases} \check{a}_{pq} = \check{a}_{pq}^R + \check{a}_{pq}^I i + \check{a}_{pq}^J j + \check{a}_{pq}^K k, & |x_p(t)|_1 \le h_p, \\ \hat{a}_{pq} = \hat{a}_{pq}^R + \hat{a}_{pq}^I i + \hat{a}_{pq}^J j + \hat{a}_{pq}^K k, & |x_p(t)|_1 > h_p, \end{cases}$$

$$b_{pq}(w_p(t)) = \begin{cases} \check{b}_{pq} = \check{b}_{pq}^R + \check{b}_{pq}^I i + \check{b}_{pq}^J j + \check{b}_{pq}^K k, & |w_p(t)|_1 \le h_p, \\ \hat{b}_{pq} = \hat{b}_{pq}^R + \hat{b}_{pq}^I i + \hat{b}_{pq}^J j + \hat{b}_{pq}^K k, & |w_p(t)|_1 > h_p, \end{cases}$$

where $\check{d}_p \ne \hat{d}_p, \check{a}_{pq} \ne \hat{a}_{pq}, \check{b}_{pq} \ne \hat{b}_{pq}, h_p^u > 0$ are the switching jump.

Definition 1. *For any $a_p \in \mathbb{Q}$, $p \in \mathbf{N}$, the fuzzy rules $\bigvee_{p\in\mathbf{N}} a_p$ and $\bigwedge_{p\in\mathbf{N}} a_p$ are defined as*

$$\begin{aligned} \bigwedge_{p\in\mathbf{N}} a_p &= \min_{p\in\mathbf{N}}\{a_p^R\} + \min_{p\in\mathbf{N}}\{a_p^I\}i + \min_{p\in\mathbf{N}}\{a_p^J\}j + \min_{p\in\mathbf{N}}\{a_p^K\}k, \\ \bigvee_{p\in\mathbf{N}} a_p &= \max_{p\in\mathbf{N}}\{a_p^R\} + \max_{p\in\mathbf{N}}\{a_p^I\}i + \max_{p\in\mathbf{N}}\{a_p^J\}j + \max_{p\in\mathbf{N}}\{a_p^K\}k. \end{aligned}$$

Remark 1. *In model (1), the fuzzy rule is introduced into QVMNN to describe the fuzzy logic in the feed-forward MAX template and feedback MIN template. Previous researchers have made efforts to compare the 'magnitude' of quaternions. For instance, Li et al. proposed a lexicographical order method [40]. In [41], the quaternion vector was decomposed into two complex-value vectors, which naturally solved the aforementioned problem using a generalized inequality technique. Additionally, the 'magnitude' of different quaternions was determined based on a defined linear distance function in [42]. In contrast to these approaches, a quaternion-valued fuzzy rule is introduced in Definition 1 in this article. Notably, Definition 1 degenerates to a real-valued fuzzy rule when $i = j = k = 0$, and to a complex-valued fuzzy rule when $j = k = 0$. This implies that the developed quaternion-valued fuzzy rule is an important generalization of its real-valued and complex-valued counterpart.*

It is worth noting that the right-hand side of system (1) is essentially discontinuous due to the presence of the switching jump points. According to the theory of non-smooth analysis in [45–48], the Filippov solution of system (1) satisfies

$$\begin{aligned} \dot{w}_p(t) \in &-\overline{co}[d_p(w_p(t))]w_p(t) + \sum_{q\in\mathbf{N}} \overline{co}[a_{pq}(w_p(t))]f_q(w_q(t)) + \sum_{q\in\mathbf{N}} \overline{co}[b_{pq}(w_p(t))]g_q(w_q(m_{pq}(t))) \\ &+ \bigvee_{q\in\mathbf{N}} \theta_{pq}g_q(w_q(m_{pq}(t))) + \bigwedge_{q\in\mathbf{N}} \sigma_{pq}g_q(w_q(m_{pq}(t))) + \sum_{q\in\mathbf{N}} c_{pq}\eta_q \\ &+ \bigvee_{q\in\mathbf{N}} \phi_{pq}\eta_q + \bigwedge_{q\in\mathbf{N}} \psi_{pq}\eta_q + \xi_p, \quad p \in \mathbf{N}, \end{aligned}$$

where the convex hull of $d_p(w_p(t))$, $a_{pq}(w_p(t))$, and $b_{pq}(w_p(t))$ are defined as

$$\overline{co}[d_p(w_p(t))] = \overline{co}[\check{d}_p^R, \hat{d}_p^R] + \overline{co}[\check{d}_p^I, \hat{d}_p^I]i + \overline{co}[\check{d}_p^J, \hat{d}_p^J]j + \overline{co}[\check{d}_p^K, \hat{d}_p^K]k,$$

$$\begin{aligned} \overline{co}[a_{pq}(w_p(t))] &= \overline{co}[\check{a}_{pq}^R, \hat{a}_{pq}^R] + \overline{co}[\check{a}_{pq}^I, \hat{a}_{pq}^I]i + \overline{co}[\check{a}_{pq}^J, \hat{a}_{pq}^J]j + \overline{co}[\check{a}_{pq}^K, \hat{a}_{pq}^K]k, \\ \overline{co}[b_{pq}(w_p(t))] &= \overline{co}[\check{b}_{pq}^R, \hat{b}_{pq}^R] + \overline{co}[\check{b}_{pq}^I, \hat{b}_{pq}^I]i + \overline{co}[\check{b}_{pq}^J, \hat{b}_{pq}^J]j + \overline{co}[\check{b}_{pq}^K, \hat{b}_{pq}^K]k. \end{aligned}$$

By the theory of measurable selections [48], there exist $\acute{d}_p(t) \in \overline{co}[d_p(w_p(t))]$, $\acute{a}_{pq}(t) \in \overline{co}[a_{pq}(w_p(t))]$, and $\acute{b}_{pq}(t) \in \overline{co}[b_{pq}(w_p(t))]$ such that

$$\begin{aligned} \dot{w}_p(t) = &-\acute{d}_p(t)w_p(t) + \sum_{q\in\mathbf{N}} \acute{a}_{pq}(t)f_q(w_q(t)) + \sum_{q\in\mathbf{N}} \acute{b}_{pq}(t)g_q(w_q(m_{pq}(t))) \\ &+ \bigvee_{q\in\mathbf{N}} \theta_{pq}g_q(w_q(m_{pq}(t))) + \bigwedge_{q\in\mathbf{N}} \sigma_{pq}g_q(w_q(m_{pq}(t))) + \sum_{q\in\mathbf{N}} c_{pq}\eta_q \\ &+ \bigvee_{q\in\mathbf{N}} \phi_{pq}\eta_q + \bigwedge_{q\in\mathbf{N}} \psi_{pq}\eta_q + \xi_p, \quad p \in \mathbf{N}. \end{aligned} \tag{2}$$

Thus, the response system of system (1) is described by

$$\begin{aligned} \dot{\delta}_p(t) = &-d_p(\delta_p(t))\delta_p(t) + \sum_{q\in\mathbf{N}} a_{pq}(\delta_p(t))f_q(\delta_q(t)) + \sum_{q\in\mathbf{N}} b_{pq}(\delta_p(t))g_q(\delta_q(m_{pq}(t))) \\ &+ \bigvee_{q\in\mathbf{N}} \theta_{pq}g_q(\delta_q(m_{pq}(t))) + \bigwedge_{q\in\mathbf{N}} \sigma_{pq}g_q(\delta_q(m_{pq}(t))) + \sum_{q\in\mathbf{N}} c_{pq}\eta_q \\ &+ \bigvee_{q\in\mathbf{N}} \phi_{pq}\eta_q + \bigwedge_{q\in\mathbf{N}} \psi_{pq}\eta_q + \xi_p + u_p(t), \quad p \in \mathbf{N}, \end{aligned} \tag{3}$$

where $u_p(t)$ is the control input and $\delta_p(s) = \daleth_p(s) \in C([-\digamma, 0])$ is the initial state of the response system (3).

Similarly, there exist $\grave{d}_p(t) \in \overline{co}[d_p(\delta_p(t))]$, $\grave{a}_{pq}(t) \in \overline{co}[a_{pq}(\delta_p(t))]$ and $\grave{b}_{pq}(t) \in \overline{co}[b_{pq}(\delta_p(t))]$ such that

$$\begin{aligned} \dot{\delta}_p(t) = &-\grave{d}_p(t)\delta_p(t) + \sum_{q\in\mathbf{N}} \grave{a}_{pq}(t)f_q(\delta_q(t)) + \sum_{q\in\mathbf{N}} \grave{b}_{pq}(t)g_q(\delta_q(m_{pq}(t))) \\ &+ \bigvee_{q\in\mathbf{N}} \theta_{pq}g_q(\delta_q(m_{pq}(t))) + \bigwedge_{q\in\mathbf{N}} \sigma_{pq}g_q(\delta_q(m_{pq}(t))) + \sum_{q\in\mathbf{N}} c_{pq}\eta_q \\ &+ \bigvee_{q\in\mathbf{N}} \phi_{pq}\eta_q + \bigwedge_{q\in\mathbf{N}} \psi_{pq}\eta_q + \xi_p + u_p(t), \quad p \in \mathbf{N}. \end{aligned} \tag{4}$$

Assumption 1. *For any $p \in \mathbf{N}$, $u, v \in \mathbb{Q}$, there exist positive constants $l_p^1, \tilde{l}_p^1, L_p^1, \tilde{L}_p^1$ such that*

$$\begin{aligned} &|f_p(u) - f_p(v)|_1 \le l_p^1|u - v|_1, \\ &|g_p(u) - g_p(v)|_1 \le \tilde{l}_p^1|u - v|_1, \\ &|f_p(u)|_1 \le L_p^1, \ \ |g_p(u)|_1 \le \tilde{L}_p^1. \end{aligned}$$

Remark 2. *Activation functions are intrinsically critical elements that affect the dynamic characteristics of the designed neural networks. According to Assumption 1, the existence and uniqueness of solutions for system (1) can be guaranteed due to the continuity of activation functions [16,17]. The assumption of Lipschitz conditions is quite common because activation functions such as the Logistic sigmoid function, piecewise linear functions, and hyperbolic tangent functions satisfy these conditions.*

Definition 2. *Drive-response QVFMNNs (1) and (3) are said to be FITS if there exist two number $T_{\max}$ and $T(\alpha(\Theta))$ satisfying $T_{\max} \ge T(\alpha(\Theta)) > 0$ such that*

$$\lim_{t\to T(\alpha(\Theta))} |\alpha(t)|_1 = 0, \ \ |\alpha(t)|_1 = 0, \ \ \textit{for all } t \ge T(\alpha(\Theta)),$$

where $\alpha(t) = (\alpha_1(t), \cdots, \alpha_p(t))^T \in \mathbb{Q}^n$, $\alpha_p(t) = \delta_p(t) - w_p(t)$, $\chi_p(s) = \varrho_p(s) - \daleth_p(s) \in C([\digamma, 0])$, $\Theta = (\delta_1(s), \cdots, \delta_p(s))^T \in \mathbb{Q}^n$, $p \in \mathbf{N}$. Moreover, drive-response QVFMNNs (1) and (3) are said to be PETS for a preassigned time T_{pat} if

$$\lim_{t\to T_{pat}} |\alpha(t)|_1 = 0, \ \ |\alpha(t)|_1 = 0, \ \ \textit{for all } t \ge T_{pat},$$

in which $T_{pat} > 0$ is completely independent of initial values and system parameters.

Definition 3. *For $o \in \mathbb{Q}$, the signum function of o is defined as*

$$[o] \triangleq sign(o^R) + isign(o^I) + jsign(o^J) + ksign(o^K).$$

For a regular, positive, and radially unbounded function $V(x) : \mathbb{Q}^n \to \mathbb{R}$, $x(t) : \mathbb{R} \to \mathbb{Q}^n$, the following results should be introduced.

Lemma 1 ([25])**.** *If there exist constants $z_1 \le 0$, $z_2 > 0$, $z_3 > 0$, $0 \le b_1 < 1$, and $b_2 > 1$ such that for any $x(t) \in \mathbb{Q}^n \setminus \{\mathbf{0_n}\}$,*

$$\frac{d}{dt}V(x(t)) \le z_1 V(x(t)) - z_2 V^{b_1}(x(t)) - z_3 V^{b_2}(x(t)),$$

then the following results are true.

(i) If $z_1 < 0$, $x(t) \equiv \mathbf{0_n}$ for $t \ge \bar{T}_1$, where

$$\bar{T}_1 = \frac{\pi}{z_2(b_2 - b_1)}\Big(\frac{z_2}{z_3}\Big)^{\varpi} csc(z_3\pi).$$

(ii) If $0 < z_1 < \min\{z_2, z_3\}$, $x(t) \equiv \mathbf{0_n}$ for $t \ge \bar{T}_2$, where

$$\begin{aligned}\bar{T}_2 = &\frac{\pi csc(\pi z_3)}{z_3(b_2 - b_1)}\Big(\frac{z_3}{z_2 - z_1}\Big)^{1-\varpi} I\Big(\frac{z_3}{z_2 + z_3 - z_1}, z_3, 1 - z_3\Big) \\ &+ \frac{\pi csc(\pi z_3)}{z_2(b_2 - b_1)}\Big(\frac{z_2}{z_3 - z_1}\Big)^{\varpi} I\Big(\frac{z_2}{z_2 + z_3 - z_1}, 1 - z_3, z_3\Big),\end{aligned}$$

in which $\varpi = (1 - b_1)/(b_2 - b_1)$ and the incomplete Beta function ratio $I(r, p, q)$ is given in [25].

(iii) If $0 < z_1 < 2\sqrt{z_2 z_3}$ and $b_1 + b_2 = 2$, $x(t) \equiv \mathbf{0_n}$ for $t \ge \bar{T}_3$, where

$$\bar{T}_3 = \frac{2}{(b_2 - 1)\sqrt{\iota}}\Big(\frac{\pi}{2} + \arctan\Big(\frac{z_1}{\iota}\Big)\Big),$$

in which $\iota = 4z_2z_3 - z_1^2$.

Lemma 2 ([25])**.** *If there exist constants $T_{pat} > 0$, $z_1 \in \mathbb{R}$, $z_2, z_3 > 0$, $0 \le b_1 < 1$, $b_2 > 1$ such that for any $x(t) \in \mathbb{Q}^n \setminus \{\mathbf{0_n}\}$,*

$$\frac{d}{dt}V(x(t)) \le -\frac{\tilde{T}}{T_{pat}}\big(-z_1 V(x(t)) + z_2 V^{b_1}(x(t)) + z_3 V^{b_2}(x(t))\big),$$

then $x(t) \equiv \mathbf{0_n}$ for $t \ge T_{pat}$, where

$$\tilde{T} = \begin{cases} \bar{T}_1, & z_1 \le 0, \\ \bar{T}_2, & 0 < z_1 < \min\{z_2, z_3\}, \\ \bar{T}_3, & 0 < z_1 < 2\sqrt{z_2 z_3}, \quad b_1 + b_2 = 2. \end{cases}$$

Lemma 3 ([25])**.** *Assume that $c_i \ge 0$ for $1 \le i \le \mathbf{N}$, $0 \le b_1 \le 1$ and $b_2 > 1$, then*

$$\sum_{i \in \mathbf{N}} c_i^{b_1} \ge \Big(\sum_{i \in \mathbf{N}} c_i\Big)^{b_1}, \quad \sum_{i \in \mathbf{N}} c_i^{b_2} \ge n^{1-b_2}\Big(\sum_{i \in \mathbf{N}} c_i\Big)^{b_2}.$$

Lemma 4 ([49])**.** *For any $\rho_1, \rho_2 \in \mathbb{Q}$, $\rho(t) : \mathbb{R} \to \mathbb{Q}$, the following properties hold*

(1) $\bar{\bar{\rho}}_1 = \rho_1$,

(2) $\rho_1 + \bar{\rho}_1 = 2\rho_1^R \le 2|\rho_1|_1$,

(3) $\overline{\rho_1\rho_2} = \overline{\rho}_2\overline{\rho}_1$,

(4) $\dfrac{d|\rho(t)|_1}{dt} = \dfrac{1}{2}(\overline{[\rho(t)]}\dfrac{d\rho(t)}{dt} + \dfrac{d\overline{\rho(t)}}{dt}[\rho(t)])$.

Lemma 5 ([49])**.** *For any $r_1, r_2, r_3 \in \mathbb{Q}$,*

$$\begin{aligned}
&(1)\ (r_1^R - |r_1^I| - |r_1^J| - |r_1^K|)|r_2|_1 \le (\overline{[r_2]}r_1r_2)^R \\
&\quad \le (r_1^R + |r_1^I| + |r_1^J| + |r_1^K|)|r_2|_1, \\
&(2)\ -|z|_1|r_3|_1 \le (\overline{[r_1]}r_2r_3)^R \le |r_2|_1|r_3|_1.
\end{aligned}$$

Lemma 6. *For any $\vartheta(t) \in \mathbb{Q}$, $D^+|\vartheta(t)|_1 \le |\dot{\vartheta}(t)|_1$.*

Proof. By Lemma 4, it can be concluded that

$$\begin{aligned}
D^+|\vartheta(t)|_1 &= \frac{1}{2}(\overline{[\vartheta(t)]}D^+\vartheta(t) + D^+\overline{\vartheta(t)}[\vartheta(t)]) \\
&= (\mathrm{sign}(\vartheta^R(t))\dot{\vartheta}^R(t) + \mathrm{sign}(\vartheta^I(t))\dot{\vartheta}^I(t) \\
&\quad + \mathrm{sign}(\vartheta^J(t))\dot{\vartheta}^J(t) + \mathrm{sign}(\vartheta^K(t))\dot{\vartheta}^K(t)) \\
&\le |\dot{\vartheta}^R(t)| + |\dot{\vartheta}^I(t)| + |\dot{\vartheta}^J(t)| + |\dot{\vartheta}^K(t)|.
\end{aligned}$$

Further, according to the definition of the absolute-based norm,

$$\begin{aligned}
|\dot{\vartheta}(t)|_1 &= |\dot{\vartheta}^R(t) + i\dot{\vartheta}^I(t) + j\dot{\vartheta}^J(t) + k\dot{\vartheta}^K(t)|_1 \\
&= |\dot{\vartheta}^R(t)| + |\dot{\vartheta}^I(t)| + |\dot{\vartheta}^J(t)| + |\dot{\vartheta}^K(t)|.
\end{aligned}$$

Thus, $D^+|\vartheta(t)|_1 \le |\dot{\vartheta}(t)|_1$. □

Lemma 7. *For any $\epsilon_p, \tilde{\epsilon}_p \in \mathbb{Q}$, $p \in \mathbf{N}$,*

$$\begin{aligned}
\Big|\bigvee_{p\in\mathbf{N}} \epsilon_p - \bigvee_{p\in\mathbf{N}} \tilde{\epsilon}_p\Big|_1 &\le \sum_{p\in\mathbf{N}} |\epsilon_p - \tilde{\epsilon}_p|_1, \\
\Big|\bigwedge_{p\in\mathbf{N}} \epsilon_p - \bigwedge_{p\in\mathbf{N}} \tilde{\epsilon}_p\Big|_1 &\le \sum_{p\in\mathbf{N}} |\epsilon_p - \tilde{\epsilon}_p|_1.
\end{aligned}$$

Proof. Based on Definition 1, there exist $\tau_1, \tau_2, \tau_3, \tau_4, \varpi_1, \varpi_2, \varpi_3, \varpi_4 \in \mathbf{N}$ such that

$$\begin{aligned}
\bigvee_{p\in\mathbf{N}} \epsilon_p &= \epsilon_{\tau_1}^R + \epsilon_{\tau_2}^I i + \epsilon_{\tau_3}^J j + \epsilon_{\tau_4}^K k, \\
\bigvee_{p\in\mathbf{N}} \tilde{\epsilon}_p &= \tilde{\epsilon}_{\varpi_1}^R + \tilde{\epsilon}_{\varpi_2}^I i + \tilde{\epsilon}_{\varpi_3}^J j + \tilde{\epsilon}_{\varpi_4}^K k.
\end{aligned}$$

Hence,

$$\begin{aligned}
&\Big|\bigvee_{p\in\mathbf{N}} \epsilon_p - \bigvee_{p\in\mathbf{N}} \tilde{\epsilon}_p\Big|_1 \\
&= |\epsilon_{\tau_1}^R - \tilde{\epsilon}_{\varpi_1}^R| + |\epsilon_{\tau_2}^I - \tilde{\epsilon}_{\varpi_2}^I| + |\epsilon_{\tau_3}^J - \tilde{\epsilon}_{\varpi_3}^J| + |\epsilon_{\tau_4}^K - \tilde{\epsilon}_{\varpi_4}^K|, \\
&\le \max\{|\epsilon_{\tau_1}^R - \tilde{\epsilon}_{\tau_1}^R|, |\epsilon_{\varpi_1}^R - \tilde{\epsilon}_{\varpi_1}^R|\} \\
&\quad + \max\{|\epsilon_{\tau_2}^I - \tilde{\epsilon}_{\tau_2}^I|, |\epsilon_{\varpi_2}^I - \tilde{\epsilon}_{\varpi_2}^I|\} \\
&\quad + \max\{|\epsilon_{\tau_3}^J - \tilde{\epsilon}_{\tau_3}^J|, |\epsilon_{\varpi_3}^J - \tilde{\epsilon}_{\varpi_3}^J|\} \\
&\quad + \max\{|\epsilon_{\tau_4}^K - \tilde{\epsilon}_{\tau_4}^K|, |\epsilon_{\varpi_4}^K - \tilde{\epsilon}_{\varpi_4}^K|\} \\
&\le \sum_{p\in\mathbf{N}} |\epsilon_p^R - \tilde{\epsilon}_p^R| + \sum_{p\in\mathbf{N}} |\epsilon_p^I - \tilde{\epsilon}_p^I|
\end{aligned}$$

$$
\begin{aligned}
&+ \sum_{p\in\mathbf{N}} |\epsilon_p^J - \tilde{\epsilon}_p^J| + \sum_{p\in\mathbf{N}} |\epsilon_p^K - \tilde{\epsilon}_p^K| \\
&\leq \sum_{p\in\mathbf{N}} |\epsilon_p - \tilde{\epsilon}_p|_1.
\end{aligned}
$$

Similar to the above analysis, it can be obtained

$$
\left| \bigwedge_{p\in\mathbf{N}} \epsilon_p - \bigwedge_{p\in\mathbf{N}} \tilde{\epsilon}_p \right|_1 \leq \sum_{p\in\mathbf{N}} |\epsilon_p - \tilde{\epsilon}_p|_1,
$$

The proof is completed. □

Remark 3. *In recent research on QVFNN [18,19,40–42], without the rigorous theoretical proof, the above two inequalities are directly used to investigate the synchronization of QVFNN. To address this gap, based on the revised fuzzy rule definition, Lemma 7 in this paper is offered.*

3. Main Results

This section presents several main theorems with an absolute-based norm and 2-norm that give the FITS and PETS of the QVFMNNs (1) and (3) by the designed event-triggered control.

3.1. FITS

Before giving the main results, several notations are provided.

$$
\begin{aligned}
\tilde{a}_{pq} &= \max\{|\hat{a}_{pq}|_1, |\check{a}_{pq}|_1\},\ \ \tilde{b}_{pq} = \max\{|\hat{b}_{pq}|_1, |\check{b}_{pq}|_1\}, \\
\tilde{d}_p &= \max\{-\hat{d}_p^R + |\hat{d}_p^I| + |\hat{d}_p^J| + |\hat{d}_p^K|, -\check{d}_p^R + |\check{d}_p^I| + |\check{d}_p^J| + |\check{d}_p^K|\}, \\
\tilde{\beta}_1 &= (2n)^{1-\varepsilon} \min_{p\in\mathbf{N}}\{\beta_p\},\ \ \tilde{\beta}_2 = (2n)^{1-\varepsilon} \min_{p\in\mathbf{N}}\{\hat{\beta}_p\},\ \ \tilde{\beta}_3 = (2n)^{1-\varepsilon} \min_{p\in\mathbf{N}}\{\check{\beta}_p\}, \\
\tilde{\kappa}_1 &= \max_{p\in\mathbf{N}}\{\tilde{d}_p + \sum_{q\in\mathbf{N}} \tilde{a}_{qp} l_p^1\},\quad \iota_1 = 4nM_1\tilde{\beta}_1 - \tilde{\kappa}_1^2,\quad \iota_2 = 4n\hat{M}_1\tilde{\beta}_2 - \tilde{\kappa}_1^2,\quad \iota_3 = 4n\check{M}_1\tilde{\beta}_3 - \tilde{\kappa}_1^2. \\
A_{1p} &= h_p^1|[\alpha_p(t)]|_1|\hat{d}_p - \check{d}_p|_1 + \sum_{q\in\mathbf{N}} \big(h_p^1|[e_p(t)]|_1|\hat{a}_{pq} - \check{a}_{pq}|_1 l_q^1 + 2\tilde{L}_q(\tilde{b}_{pq}|[\alpha_p(t)]|_1 + |\theta_{pq}|_1 + |\sigma_{pq}|_1)\big), \\
A_{2p} &= h_p^1|[\alpha_p(t)]|_1|\hat{d}_p - \check{d}_p|_1 + \sum_{q\in\mathbf{N}} \big(l_q^1 h_p^1|[\alpha_p(t)]|_1|\hat{a}_{pq} - \check{a}_{pq}|_1 + 2\tilde{L}_q\tilde{b}_{pq}|[\alpha_p(t)]|_1\big), \\
A_{3p} &= \tilde{d}_p h_p^1 + \sum_{q\in\mathbf{N}} \big(\tilde{a}_{pq} l_q^1 h_q^1 + 2\tilde{L}_q(\tilde{b}_{pq}|[\alpha_p(t)]|_1 + |\theta_{pq}|_1 + |\sigma_{pq}|_1)\big).
\end{aligned}
$$

To achieve FITS, the event-triggered controller based on the absolute-based norm is designed by

$$
u_p(t) = -[\alpha_p(t_s)](\gamma_p + \beta_p|\alpha_p(t_s)|_1^{\varepsilon}),\ \ t \in [t_s, t_{s+1}), \tag{5}
$$

where $t_s, s \in \mathbb{Z}$ is the latest triggering instant with $t_0 = 0$, $\varepsilon > 1$, and γ_p, β_p are positive constants, $p \in \mathbf{N}$.

The dynamic triggering law are developed as follows

$$
\begin{cases}
t_{s+1} = \inf\{t : t \geq t_s, F_p(t) \geq 0\}, \\
F_p(t) = A_{1p} + |E_p(t)|_1 - \gamma_p + M_1 - \daleth_p\lambda_p(t), \\
\dot{\lambda}_p(t) = -\daleth_p\lambda_p(t) - \beta_p\lambda_p^{\varepsilon}(t),
\end{cases} \tag{6}
$$

where $M_1, \beth_p > 0$ and $\lambda_p(t)$ with $\lambda_p(0) > 0$ is the internal dynamic variable and $E_p(t)$ is the measure errors and described by

$$E_p(t) = [\alpha_p(t_s)](\gamma_p + \beta_p|\alpha_p(t_s)|_1^\varepsilon) - [\alpha_p(t)](\gamma_p + \beta_p|\alpha_p(t)|_1^\varepsilon).$$

The above event-triggered synchronization mechanism is shown in Figure 1.

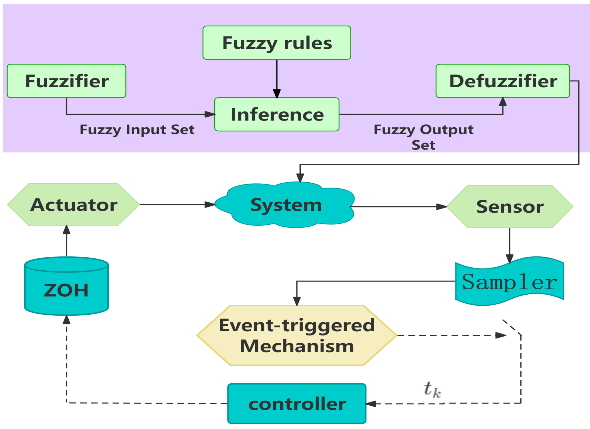

Figure 1. Structure of FMQVNNs with event-triggered control mechanism.

Lemma 8. *For any $t \geq 0$, $p \in \mathbb{N}$, $\lambda_p(t) \geq 0$.*

Proof. To begin with, confirm that $\lambda_p(t) \geq 0$ is valid for any $t \geq 0$. If it is not valid, there exists a $\tilde{t}$ such that $\lambda_p(\tilde{t}) < 0$. Since $\lambda_p(t)$ with $\lambda_p(0) > 0$ is continuous, there exist some $\hat{t}$ in the interval $(0, \tilde{t})$ such that $\lambda_p(\hat{t}) = 0$. Let $t^* = \inf\{\hat{t}|\lambda_p(\hat{t}) = 0, \hat{t} \in (0, \tilde{t})\}$. Obviously, $\lambda_p(t^*) = 0$ and $\lambda_p(t) > 0$ for $t \in [0, t^*)$.

Integrate both sides of the third term in (6) to obtain

$$0 = \lambda_p(t^*) = e^{\int_0^{t^*}(-\beth_p - \beta_p \lambda_p^{\varepsilon-1}(t))ds}\lambda_p(0) > 0,$$

this is contradictory to the above conditions. Therefore, for any $t \geq 0$, $\lambda_p(t) \geq 0$. □

Remark 4. *In comparison to traditional static event-triggering mechanisms [43,44], the key advantage of dynamic event-triggering mechanisms is that they can adjust the triggering conditions based on the current state and performance requirements of the system, thereby adapting to the constantly changing system environment and demands. This paper introduces a dynamic variable function $\lambda_p(t)$ into the event-triggering conditions, which can converge from $\lambda_p(0)$ to 0 over time. Such a design allows for dynamic adjustment of the triggering threshold according to changes in the system state. As a result, it can help to reduce the number of data packet transmissions and thus lower the likelihood of network congestion. Furthermore, the dynamic event-triggering mechanism can also reduce unnecessary task execution, save computational resources, and decrease energy consumption.*

Theorem 1. *Based on Assumption 1 the event-triggered control mechanism (5) and (6), then the following results are true.*

(1) If $\tilde{k}_1 \leq 0$, the FITS of QVFMNNs (1) and (3) can be realized and the ST is estimated by

$$T_1 = \frac{\pi}{\varepsilon n M_1}(\frac{nM_1}{\tilde{\beta}_1})^{\frac{1}{\varepsilon}}\csc(\frac{\pi}{\varepsilon}).$$

(2) *If* $0 < \tilde{k}_1 < \min\{nM_1, \tilde{\beta}_1\}$, *then* $\alpha(t) \equiv \mathbf{0_n}$ *for* $t \geq T_2$, *in which*

$$T_2 = \frac{\pi csc(\pi\varepsilon)}{\tilde{\beta}_1\hat{\varepsilon}}(\frac{\tilde{\beta}_1}{nM_1 - \tilde{k}_1})^{1-\hat{\varepsilon}} I(\frac{\tilde{\beta}_1}{nM_1 + \tilde{\beta}_1 - \tilde{k}_1}, \varepsilon, 1-\hat{\varepsilon}) + \frac{\pi csc(\pi\varepsilon)}{nM_1\hat{\varepsilon}}(\frac{nM_1}{\tilde{\beta}_2 - \tilde{k}_1})^{\hat{\varepsilon}} I(\frac{nM_1}{nM_1 + \tilde{\beta}_2 - \tilde{k}_1}, 1-\hat{\varepsilon}, \hat{\varepsilon}).$$

(3) *If* $0 < \tilde{k}_1 < 2\sqrt{nM_1\tilde{\beta}_1}$ *and* $\varepsilon = 2$, *then* $\alpha(t) \equiv \mathbf{0_n}$ *for* $t \geq T_3$, *in which*

$$T_3 = \frac{2}{\sqrt{\iota_1}}(\frac{\pi}{2} + \arctan(\frac{\tilde{k}_1}{\iota_1})).$$

Proof. Consider the following absolute-based norm Lyapunov function

$$V(t) = V_1(t) + V_2(t) = \sum_{p\in\mathbf{N}} |\alpha_p(t)|_1 + \sum_{p\in\mathbf{N}} \lambda_p(t).$$

According to the systems (1) and (3), for any $\alpha(t) \in \mathbb{R}^n \setminus \{\mathbf{0_n}\}$,

$$\begin{aligned}
D^+V_1(t) = &\frac{1}{2}\sum_{p\in\mathbf{N}}(\overline{[\alpha_p(t)]}D^+\alpha_p(t) + D^+\overline{\alpha_p(t)}[\alpha_p(t)]) \\
= &-\frac{1}{2}\sum_{p\in\mathbf{N}}\Big(\overline{[\alpha_p(t)]}(\grave{d}_p(t)\delta_p(t) - \acute{d}_p(t)w_p(t)) \\
&- \overline{(\grave{d}_p(t)\delta_p(t) - \acute{d}_p(t)w_p(t))}[\alpha_p(t)]\Big) \\
&+ \frac{1}{2}\sum_{p\in\mathbf{N}}\sum_{q\in\mathbf{N}}\Big(\overline{[\alpha_p(t)]}(\grave{a}_{pq}(t)f_q(\delta_q(t)) - \acute{a}_{pq}(t)f_q(w_q(t))) \\
&+ \overline{(\grave{a}_{pq}(t)f_q(\delta_q(t)) - \acute{a}_{pq}(t)f_q(w_q(t)))}[\alpha_p(t)]\Big) \\
&+ \frac{1}{2}\sum_{p\in\mathbf{N}}\sum_{q\in\mathbf{N}}\Big(\overline{[\alpha_p(t)]}(\grave{b}_{pq}(t)g_q(\delta_q(m_{pq}(t))) - \acute{b}_{pq}(t)g_q(w_q(m_{pq}(t)))) \\
&+ \overline{(\grave{b}_{pq}(t)g_q(\delta_q(m_{pq}(t))) - \acute{b}_{pq}(t)g_q(w_q(m_{pq}(t))))}[\alpha_p(t)]\Big) \\
&+ \frac{1}{2}\sum_{p\in\mathbf{N}}\Big(\overline{[\alpha_p(t)]}(\bigvee_{q\in\mathbf{N}}\theta_{pq}g_q(\delta_q(m_{pq}(t)))) - \bigvee_{q\in\mathbf{N}}\theta_{pq}g_q(w_q(m_{pq}(t)))) \\
&+ \overline{\bigvee_{q\in\mathbf{N}}\theta_{pq}g_q(\delta_q(m_{pq}(t)))) - \bigvee_{q\in\mathbf{N}}\theta_{pq}g_q(w_q(m_{pq}(t)))}[\alpha_p(t)]\Big) \\
&+ \frac{1}{2}\sum_{p\in\mathbf{N}}\Big(\overline{[\alpha_p(t)]}(\bigwedge_{q\in\mathbf{N}}\sigma_{pq}g_q(\delta_q(m_{pq}(t)))) - \bigwedge_{q\in\mathbf{N}}\sigma_{pq}g_q(w_q(m_{pq}(t)))) \\
&+ \overline{\bigwedge_{q\in\mathbf{N}}\sigma_{pq}g_q(\delta_q(m_{pq}(t)))) - \bigwedge_{q\in\mathbf{N}}\sigma_{pq}g_q(w_q(m_{pq}(t)))}[\alpha_p(t)]\Big) \\
&+ \frac{1}{2}\sum_{p\in\mathbf{N}}\Big(\overline{[\alpha_p(t)]}u_p(t) + \overline{u_p(t)}[\alpha_p(t)]\Big).
\end{aligned} \tag{7}$$

when $\alpha(t) \neq \{\mathbf{0_n}\}$, based on Lemma 4,

$$-\frac{1}{2}\sum_{p\in\mathbf{N}}\Big(\overline{\alpha_p(t)}(\grave{d}_p(t)\delta_p(t) - \acute{d}_p(t)w_p(t)) - \overline{(\grave{d}_p(t)\delta_p(t) - \acute{d}_p(t)w_p(t))}\alpha_p(t)\Big)$$

$$= -\sum_{p\in\mathbf{N}} \left\{ \alpha_p(t)(\grave{d}_p(t)\delta_p(t) - \acute{d}_p(t)w_p(t)) \right\}^R.$$

In view of Lemma 5, the following cases are discussed.

(1) When $|w_p(t)|_1$, $|\delta_p(t)|_1 \le h_p^1$,

$$\begin{aligned}
&-\sum_{p\in\mathbf{N}} \left\{ [\alpha_p(t)](\grave{d}_p(t)\delta_p(t) - \acute{d}_p(t)w_p(t)) \right\}^R \\
&= -\sum_{p\in\mathbf{N}} \left\{ [\alpha_p(t)]\check{d}_p\alpha_p(t) \right\}^R \\
&\le \sum_{p\in\mathbf{N}} (-\check{d}_p^R + |\check{d}_p I| + |\check{d}_p^J| + |\check{d}_p^K|)|\alpha_p(t)|_1.
\end{aligned}$$

(2) When $|w_p(t)|_1$, $|\delta_p(t)|_1 > h_p^1$,

$$\begin{aligned}
&-\sum_{p\in\mathbf{N}} \left\{ [\alpha_p(t)](\grave{d}_p(t)\delta_p(t) - \acute{d}_p(t)w_p(t)) \right\}^R \\
&= -\sum_{p\in\mathbf{N}} \left\{ [\alpha_p(t)]\hat{d}_p\alpha_p(t) \right\}^R \\
&\le \sum_{p\in\mathbf{N}} (-\hat{d}_p^R + |\hat{d}_p I| + |\hat{d}_p^J| + |\hat{d}_p^K|)|\alpha_p(t)|_1.
\end{aligned}$$

(3) When $|w_p(t)|_1 > h_p^1$, $|\delta_p(t)|_1 \le h_p^1$,

$$\begin{aligned}
&-\sum_{p\in\mathbf{N}} \left\{ [\alpha_p(t)](\grave{d}_p(t)\delta_p(t) - \acute{d}_p(t)w_p(t)) \right\}^R \\
&= -\sum_{p\in\mathbf{N}} \left\{ [e_p(t)](\check{d}_p\delta_p(t) - \hat{d}_p w_p(t)) \right\}^R \\
&= -\sum_{p\in\mathbf{N}} \left\{ [e_p(t)](\check{d}_p\delta_p(t) - \hat{d}_p\delta_p(t) + \hat{d}_p\delta_p(t) - \hat{d}_p w_p(t)) \right\}^R \\
&\le \sum_{p\in\mathbf{N}} (-\hat{d}_p^R + |\hat{d}_p I| + |\hat{d}_p^J| + |\hat{d}_p^K|)|\alpha_p(t)|_1 + h_p^1|[\alpha_p(t)]|_1|\hat{d}_p - \check{d}_p|_1.
\end{aligned}$$

(4) When $|w_p(t)|_1 \le h_p^1$, $|\delta_p(t)|_1 > h_p^1$,

$$\begin{aligned}
&-\sum_{p\in\mathbf{N}} \left\{ [\alpha_p(t)](\grave{d}_p(t)\delta_p(t) - \acute{d}_p(t)w_p(t)) \right\}^R \\
&= -\sum_{p\in\mathbf{N}} \left\{ [\alpha_p(t)](\hat{d}_p\delta_p(t) - \check{d}_p w_p(t)) \right\}^R \\
&= -\sum_{p\in\mathbf{N}} \left\{ [\alpha_p(t)](\hat{d}_p\delta_p(t) - \hat{d}_p w_p(t) + \hat{d}_p w_p(t) - \check{d}_p w_p(t)) \right\}^R \\
&\le \sum_{p\in\mathbf{N}} (-\hat{d}_p^R + |\hat{d}_p I| + |\hat{d}_p^J| + |\hat{d}_p^K|)|\alpha_p(t)|_1 + h_p^1|[\alpha_p(t)]|_1|\hat{d}_p - \check{d}_p|_1.
\end{aligned}$$

As mentioned above,

$$-\frac{1}{2}\sum_{p\in\mathbf{N}} \left(\overline{[\alpha_p(t)]}(\grave{d}_p(t)\delta_p(t) - \acute{d}_p(t)w_p(t)) - \overline{(\grave{d}_p(t)\delta_p(t) - \acute{d}_p(t)w_p(t))}[\alpha_p(t)] \right)$$

$$\leq \sum_{p\in\mathbf{N}} \tilde{d}_p|\alpha_p(t)|_1 + h_p^1|[\alpha_p(t)]|_1|\hat{d}_p - \check{d}_p|_1. \tag{8}$$

From Assumption 1,

$$\begin{aligned}
&\frac{1}{2}\sum_{p\in\mathbf{N}}\sum_{q\in\mathbf{N}}\Big(\overline{[\alpha_p(t)]}(\grave{a}_{pq}(t)f_q(\delta_q(t)) - \acute{a}_{pq}(t)f_q(w_q(t)))\\
&+\overline{(\grave{a}_{pq}(t)f_q(\delta_q(t)) - a_{pq}(w_p(t))f_q(w_q(t)))}[\alpha_p(t)]\Big)\\
\leq &\sum_{p\in\mathbf{N}}\sum_{q\in\mathbf{N}}(l_p\tilde{a}_{qp}|\alpha_p(t)|_1 + l_q h_p^1|[\alpha_p(t)]|_1|\hat{a}_{pq} - \check{a}_{pq}|_1),
\end{aligned} \tag{9}$$

and

$$\begin{aligned}
&\frac{1}{2}\sum_{p\in\mathbf{N}}\sum_{q\in\mathbf{N}}\Big(\overline{[\alpha_p(t)]}(\grave{b}_{pq}(t)g_q(\delta_q(m_{pq}(t))) - \acute{b}_{pq}(t)g_q(w_q(m_{pq}(t))))\\
&+\overline{(\grave{b}_{pq}(t)g_q(\delta_q(m_{pq}(t))) - \acute{b}_{pq}(t)g_q(w_q(m_{pq}(t))))}[\alpha_p(t)]\Big)\\
\leq &\sum_{p\in\mathbf{N}}\sum_{q\in\mathbf{N}}2\tilde{b}_{pq}\tilde{L}_q|[\alpha_p(t)]|_1.
\end{aligned} \tag{10}$$

In addition, in light of Lemma 7,

$$\begin{aligned}
&\frac{1}{2}\sum_{p\in\mathbf{N}}\Big(\overline{[\alpha_p(t)]}(\bigvee_{q\in\mathbf{N}}\theta_{pq}g_q(\delta_q(m_{pq}(t)))) - \bigvee_{q\in\mathbf{N}}\theta_{pq}g_q(w_q(m_{pq}(t))))\\
&+\overline{\bigvee_{q\in\mathbf{N}}\theta_{pq}g_q(\delta_q(m_{pq}(t)))) - \bigvee_{q\in\mathbf{N}}\theta_{pq}g_q(w_q(m_{pq}(t)))}[\alpha_p(t)]\Big)\\
\leq &\sum_{p\in\mathbf{N}}\sum_{q\in\mathbf{N}}2|\theta_{pq}|_1\tilde{L}_q,
\end{aligned} \tag{11}$$

and

$$\begin{aligned}
&\frac{1}{2}\sum_{p\in\mathbf{N}}\Big(\overline{[\alpha_p(t)]}(\bigwedge_{q\in\mathbf{N}}\sigma_{pq}g_q(\delta_q(m_{pq}(t)))) - \bigwedge_{q\in\mathbf{N}}\sigma_{pq}g_q(w_q(m_{pq}(t))))\\
&+\overline{\bigwedge_{q\in\mathbf{N}}\sigma_{pq}g_q(\delta_q(m_{pq}(t)))) - \bigwedge_{q\in\mathbf{N}}\sigma_{pq}g_q(w_q(m_{pq}(t)))}[\alpha_p(t)]\Big)\\
\leq &\sum_{p\in\mathbf{N}}\sum_{q\in\mathbf{N}}2|\sigma_{pq}|_1\tilde{L}_q.
\end{aligned} \tag{12}$$

From event-triggered mechanism (5) and (6), for any $\alpha(t) \in \mathbb{Q}^n \setminus \{\mathbf{0_n}\}$,

$$\begin{aligned}
&\frac{1}{2}\sum_{p\in\mathbf{N}}\Big(\overline{[\alpha_p(t)]}u_p(t) + \overline{u_p(t)}[\alpha_p(t)]\Big)\\
= &-\frac{1}{2}\sum_{p\in\mathbf{N}}([\overline{\alpha_p(t)}]E_p(t) + \overline{E_p(t)}[\alpha_p(t)]) - \sum_{p\in\mathbf{N}}[\overline{\alpha_p(t)}][\alpha_p(t)]\gamma_p\\
&-\sum_{p\in\mathbf{N}}[\overline{\alpha_p(t)}][\alpha_p(t)]\beta_p|\alpha_p(t)|_1^{\varepsilon}\\
\leq &\sum_{p\in\mathbf{N}}(|E_p(t)|_1 - \gamma_p - \beta_p|\alpha_p(t)|_1^{\varepsilon}).
\end{aligned} \tag{13}$$

Submitting the (8)–(13) into (7) and using the event-triggered condition (6),

$$
\begin{aligned}
D^{+}V_1(t) \leq & \sum_{p\in\mathbf{N}}(\tilde{d}_p+\sum_{q\in\mathbf{N}}l_p\tilde{a}_{qp})|\alpha_p(t)|_1-\sum_{p\in\mathbf{N}}\beta_p|\alpha_p(t)|_1^{\varepsilon} \\
& +\sum_{p\in\mathbf{N}}(A_{1p}+|E_p(t)|_1-\gamma_p) \\
\leq & \sum_{p\in\mathbf{N}}(\tilde{d}_p+\sum_{q\in\mathbf{N}}l_p\tilde{a}_{qp})|\alpha_p(t)|_1-\sum_{p\in\mathbf{N}}\beta_p|\alpha_p(t)|_1^{\varepsilon}-nM_1 \\
= & \tilde{\kappa}_1\sum_{p\in\mathbf{N}}|\alpha_p(t)|_1-\sum_{p\in\mathbf{N}}\beta_p|\alpha_p(t)|_1^{\varepsilon}+\sum_{p\in\mathbf{N}}\beta_p\lambda_p(t)^{\varepsilon}-nM_1.
\end{aligned}
$$

If $\tilde{k}_1 \leq 0$,

$$
D^{+}V(t) \leq -\tilde{\beta}_1 V^{\varepsilon}(t)-nM_1,
$$

according to Lemma 1, the QVFMNNs (1) and (3) are fixed-time synchronized within the time T_1.

When $0<\tilde{k}_1<\min\{nM_1,\tilde{\beta}_1\}$,

$$
D^{+}V(t) \leq \tilde{\kappa}_1 V(t)-\tilde{\beta}_1 V^{\varepsilon}(t)-nM_1,
$$

the QVFMNNs (1) and (3) can realize FXT synchronization within the time T_2. In particular, when $0<\tilde{k}_1<2\sqrt{nM_1\tilde{\beta}_1}$, the FITS of QVFMNNs (1) and (3) will be achieved within the time T_3. The proof is complied. □

Remark 5. *In [40,41], researchers explored the dissipativity and synchronicity of QVFMNNs employing the quadratic norm methodology. Contrarily, our investigation diverges from these prior studies by concentrating on the fixed-time synchronization of QVFMNNs via the 1-norm perspective. This method not only provides more accurate estimations of system settling times but also broadens the scope of our conclusions. As a result, our study gains applicability across a wider array of systems.*

It is worth noting that if the fuzzy terms are removed, system (1) will degenerate into the following QVMNN,

$$
\begin{aligned}
\dot{w}_p(t) = & -d_p(w_p(t))w_p(t)+\sum_{q\in\mathbf{N}}a_{pq}(w_p(t))f_q(w_q(t)) \\
& +\sum_{q\in\mathbf{N}}b_{pq}(w_p(t))g_q(w_q(m_{pq}(t)))+\xi_p, \quad q\in\mathbf{N},
\end{aligned} \tag{14}
$$

Correspondingly, the response system is degenerated to

$$
\begin{aligned}
\dot{\delta}_p(t) = & -d_p(\delta_p(t))\delta_p(t)+\sum_{q\in\mathbf{N}}a_{pq}(\delta_p(t))f_q(\delta_q(t)) \\
& +\sum_{q\in\mathbf{N}}b_{pq}(\delta_p(t))g_q(\delta_q(m_{pq}(t)))+\xi_p+\hat{u}_p(t), \quad q\in\mathbf{N}.
\end{aligned} \tag{15}
$$

In order to realize the FITS of QVMNNs (14) and (15), the following event-triggered controller is designed for all $t\in[t_{\hat{s}},t_{\hat{s}+1})$,

$$
\hat{u}_p(t)=-[\alpha_p(t_{\hat{s}})](\hat{\gamma}_p+\hat{\beta}_p|\alpha_p(t_{\hat{s}})|_1^{\hat{\varepsilon}}), \tag{16}
$$

where $t_{\hat{s}},\hat{s}\in\mathbb{Z}$ is the latest triggering instant with $t_0=0$ and $\hat{\varepsilon}>1$ and $\hat{\gamma}_p$, $\hat{\beta}_p$ are positive constants, $p\in\mathbb{N}$.

The triggering condition is developed by

$$\begin{cases} t_{\hat{s}+1} = \inf\{t : t \geq t_{\hat{s}}, \hat{F}_p(t) \geq 0\}, \\ \hat{F}_p(t) = A_{2p} + |\hat{E}_p(t)|_1 - \hat{\gamma}_p + \hat{M}_1 - \hat{\beth}_p \hat{\lambda}_p(t), \\ \dot{\hat{\lambda}}_p(t) = -\hat{\beth}_p \hat{\lambda}_p(t) - \hat{\beta}_p \hat{\lambda}_p^{\hat{\varepsilon}}(t), \end{cases} \tag{17}$$

where $\hat{M}_1, \hat{\beth}_p > 0$, $\hat{\lambda}(t)$ with $\hat{\lambda}_p(0) > 0$ is the internal dynamic variable and $\hat{E}_p(t)$ is the measure errors and described by

$$\hat{E}_p(t) = [\alpha_p(t_{\hat{s}})](\hat{\gamma}_p + \hat{\beta}_p |\alpha_p(t_{\hat{s}})|_1^{\hat{\varepsilon}}) - [\alpha_p(t)](\hat{\gamma}_p + \hat{\beta}_p |\alpha_p(t)|_1^{\hat{\varepsilon}}).$$

Corollary 1. *According to Assumption 1, the event-triggered control mechanism (16) and (17), then the following results are true.*

(1) *If $\tilde{k}_1 \leq 0$, the FITS of systems (14) and (15) can be realized and the ST is estimated by*

$$\hat{T}_1 = \frac{\pi}{\hat{\varepsilon} n \hat{M}} \left(\frac{n\hat{M}_1}{\tilde{\beta}_2}\right)^{\frac{1}{\hat{\varepsilon}}} \csc\left(\frac{\pi}{\hat{\varepsilon}}\right).$$

(2) *If $0 < \tilde{k}_1 < \min\{n\hat{M}_1, \tilde{\beta}_2\}$, then $\alpha(t) \equiv \mathbf{0_n}$ for $t \geq \hat{T}_2$, where*

$$\hat{T}_2 = \frac{\pi csc(\pi\hat{\varepsilon})}{\tilde{\beta}_2 \hat{\varepsilon}} \left(\frac{\tilde{\beta}_2}{n\hat{M}_1 - \tilde{k}_1}\right)^{1-\hat{\varepsilon}} I\left(\frac{\tilde{\beta}_2}{n\hat{M}_1 + \tilde{\beta}_2 - \tilde{k}_1}, \hat{\varepsilon}, 1-\hat{\varepsilon}\right) + \frac{\pi csc(\pi\hat{\varepsilon})}{n\hat{M}_1 \hat{\varepsilon}} \left(\frac{n\hat{M}_1}{\tilde{\beta}_2 - \tilde{k}_1}\right)^{\hat{\varepsilon}} I\left(\frac{\varepsilon}{\hat{\varepsilon} + \tilde{\beta}_2 - \tilde{k}_1}, 1-\hat{\varepsilon}, \hat{\varepsilon}\right).$$

(3) *If $0 < \tilde{k}_1 < 2\sqrt{\hat{\varepsilon}\tilde{\beta}_2}$ and $\hat{\varepsilon} = 2$, then $\alpha(t) \equiv \mathbf{0_n}$ for $t \geq \hat{T}_3$, where*

$$\hat{T}_3 = \frac{2}{\sqrt{\iota_2}} \left(\frac{\pi}{2} + \arctan\left(\frac{\tilde{k}_1}{\iota_2}\right)\right).$$

On the other hand, if the memristive mechanisms are removed, system (1) will degenerate into QVMNN,

$$\begin{aligned} \dot{w}_p(t) = & -d_p w_p(t) + \sum_{q\in\mathbf{N}} a_{pq} f_q(w_q(t)) + \sum_{q\in\mathbf{N}} b_{pq} g_q(w_q(m_{pq}(t))) + \sum_{q\in\mathbf{N}} c_{pq}\lambda_q \\ & + \bigvee_{q\in\mathbf{N}} \theta_{pq} g_q(w_q(m_{pq}(t))) + \bigwedge_{q\in\mathbf{N}} \sigma_{pq} g_q(w_q(m_{pq}(t))) \\ & + \bigvee_{q\in\mathbf{N}} \phi_{pq}\lambda_q + \bigwedge_{q\in\mathbf{N}} \psi_{pq}\lambda_q + \xi_p, \quad q \in \mathbf{N}, \end{aligned} \tag{18}$$

Similarly, the response system is given by

$$\begin{aligned} \dot{\delta}_p(t) = & -d_p \delta_p(t) + \sum_{q\in\mathbf{N}} a_{pq} f_q(\delta_q(t)) + \sum_{q\in\mathbf{N}} b_{pq} g_q(\delta_q(m_{pq}(t))) + \sum_{q\in\mathbf{N}} c_{pq}\lambda_q \\ & + \bigvee_{q\in\mathbf{N}} \theta_{pq} g_q(\delta_q(m_{pq}(t))) + \bigwedge_{q\in\mathbf{N}} \sigma_{pq} g_q(\delta_q(m_{pq}(t))) \\ & + \bigvee_{q\in\mathbf{N}} \phi_{pq}\lambda_q + \bigwedge_{q\in\mathbf{N}} \psi_{pq}\lambda_q + \xi_p + \check{u}_p(t), \quad q \in \mathbf{N}, \end{aligned} \tag{19}$$

In order to realize the FITS of QVMNNs (18) and (19), the following event-triggered controller is designed for all $t \in [t_{\check{s}}, t_{\check{s}+1})$,

$$\check{u}_p(t) = -[\alpha_p(t_{\check{s}})](\check{\gamma}_p + \check{\beta}_p |\alpha_p(t_{\check{s}})|_1^{\check{\varepsilon}}), \tag{20}$$

where $t_{\check{s}}, \check{s} \in \mathbb{Z}$ is the latest triggering instant with $t_0 = 0$, $\check{\varepsilon} > 1$ and $\check{\gamma}_p$, $\check{\beta}_p$ are positive constants, $p \in \mathbf{N}$.

The triggering condition is developed as follows

$$\begin{cases} t_{\check{s}+1} = \inf\{t : t \geq t_{\check{s}}, \check{F}_p(t) \geq 0\}, \\ \check{F}_p(t) = A_{2p} + |\check{E}_p(t)|_1 - \check{\gamma}_p + \check{M}_1 - \check{\beth}_p \check{\lambda}_p(t), \\ \dot{\check{\lambda}}_p(t) = -\check{\beth}_p \check{\lambda}_p(t) - \check{\beta}_p \check{\lambda}_p^{\check{\varepsilon}}(t), \end{cases} \tag{21}$$

where $\check{M}_1, \check{\beth}_p > 0$, $\check{\lambda}(t)$ with $\check{\lambda}_p(0) > 0$ is the internal dynamic variable and $\check{E}_p(t)$ is the measure errors and described by

$$\check{E}_p(t) = [\alpha_p(t_{\check{s}})](\check{\gamma}_p + \check{\beta}_p |\alpha_p(t_{\check{s}})|_1^{\check{\varepsilon}}) - [\alpha_p(t)](\check{\gamma}_p + \check{\beta}_p |\alpha_p(t)|_1^{\check{\varepsilon}}).$$

Corollary 2. *Based on Assumption 1, the event-triggered control mechanism (20) and (21), then the following results are true.*

(1) If $\tilde{k}_1 \leq 0$, the FITS of systems (18) and (19) can be realized and the ST is estimated by

$$\check{T}_1 = \frac{\pi}{\check{\varepsilon} n \check{M}_1} (\frac{n\check{M}_1}{\tilde{\beta}_3})^{\frac{1}{\check{\varepsilon}}} \csc(\frac{\pi}{\check{\varepsilon}}).$$

(2) If $0 < \tilde{k}_1 < \min\{n\check{M}_1, \tilde{\beta}_3\}$, then $\alpha(t) \equiv \mathbf{0_n}$ for $t \geq \check{T}_2$, where

$$\begin{aligned} \check{T}_2 = & \frac{\pi csc(\pi\check{\varepsilon})}{\tilde{\beta}_3 \check{\varepsilon}} (\frac{\tilde{\beta}_3}{n\check{M}_1 - \tilde{k}_1})^{1-\check{\varepsilon}} I(\frac{\tilde{\beta}_3}{n\check{M}_1 + \tilde{\beta}_3 - \tilde{k}_1}, \check{\varepsilon}, 1-\check{\varepsilon}) \\ & + \frac{\pi csc(\pi\check{\varepsilon})}{n\check{M}_1 \check{\varepsilon}} (\frac{n\check{M}_1}{\tilde{\beta}_3 - \tilde{k}_1})^{\check{\varepsilon}} I(\frac{\check{\varepsilon}}{\check{\varepsilon} + \tilde{\beta}_3 - \tilde{k}_1}, 1-\check{\varepsilon}, \check{\varepsilon}). \end{aligned}$$

(3) If $0 < \tilde{k}_1 < 2\sqrt{\check{\varepsilon}\tilde{\beta}_3}$ and $\check{\varepsilon} = 2$, then $\alpha(t) \equiv \mathbf{0_n}$ for $t \geq \check{T}_3$, where

$$\check{T}_3 = \frac{2}{\sqrt{\iota_3}} (\frac{\pi}{2} + \arctan(\frac{\tilde{k}_1}{\iota_3})).$$

Remark 6. *Based on Corollaries 1 and 2, the following results can be obtained. Firstly, the authors investigated the issues of FITS and PETS for QVNNs [13]. If the system in this paper is degenerated, the FITS and PETS of QVNNs based on event-triggered control can be achieved. Secondly, compared to the asymptotic synchronization results of the QVMNNs in [15–17], if the fuzzy mechanism in the system of this paper is removed, the FITS and PETS of the systems can be obtained. Lastly, if the system in this paper is reduced to a QVFNN, better synchronization results can be obtained as compared to [19].*

Next, we will prove that Zeno behavior does not occur under the designed event-triggering mechanism. For convenience, let

$$\begin{aligned} B_1 = & |\hat{d}_p - \check{d}_p|_1 h_p^1 |\alpha_p(t)|_1 + 2\sum_{q \in \mathbf{N}} |\tilde{a}_{pq}|_1 L_q^1 |\alpha_p(t)|_1 \\ & + 2\sum_{q \in \mathbf{N}} |\tilde{b}_{pq}|_1 \tilde{L}_q^1 |\alpha_p(t)|_1 + 2\sum_{q \in \mathbf{N}} |\theta_{pq}|_1 \tilde{L}_q^1 \\ & + 2\sum_{q \in \mathbf{N}} |\sigma_{pq}|_1 \tilde{L}_q^1 + 4\gamma_p. \end{aligned}$$

Theorem 2. *Based on the event-triggered controller mechanism (5) and (6), there is no Zeno behavior in systems (1) and (3).*

Proof. From Theorem 1, $\dot{V}_1(t) \leq 0$, which leads to

$$|\alpha_p(t)|_1 \leq \sum_{p\in\mathbf{N}} |\alpha_p(t)|_1 = V_1(t) \leq V_1(0) = G_1.$$

Consider the Dini derivative of $|E_p(t)|_1$,

$$\begin{aligned} D^+|E_p(t)|_1 &= \frac{1}{2}([\overline{E_p(t)}]D^+E_p(t) + D^+\overline{E_p(t)}[E_p(t)]) \\ &= \frac{1}{2}\Big\{[\overline{E_p(t)}][\alpha_p(t)](-\beta_p\varepsilon|\alpha_p(t)|_1^{\varepsilon-1}D^+|\alpha_p(t)|_1) \\ &\quad + [\overline{\alpha_p(t)}](-\beta_p\varepsilon|\alpha_p(t)|_1^{\varepsilon-1}D^+|\alpha_p(t)|_1)[E_p(t)]\Big\} \\ &\leq 4\beta_p\varepsilon|\alpha_p(t)|_1^{\varepsilon-1}|D^+|\alpha_p(t)|_1|, \end{aligned}$$

By Lemma 6, for any $t \in [t_s, t_{s+1})$,

$$\begin{aligned} D^+|\alpha_p(t)|_1 &\leq |\dot{\alpha}_p(t)|_1 \\ &\leq |\tilde{d}_p|_1|\alpha_p(t)|_1 + |\hat{d}_p - \check{d}_p|_1 h_p^1|\alpha_p(t)|_1 + 2\sum_{q\in\mathbf{N}}|\tilde{a}_{pq}|_1 L_q^1|\alpha_p(t)|_1 + 2\sum_{q\in\mathbf{N}}|\tilde{b}_{pq}|_1\tilde{L}_q^1|\alpha_p(t)|_1 \\ &\quad + 2\sum_{q\in\mathbf{N}}|\theta_{pq}|_1\tilde{L}_q^1 + 2\sum_{q\in\mathbf{N}}|\sigma_{pq}|_1\tilde{L}_q^1 + 4(\gamma_p + \beta_p|\alpha_p(t_s)|_1^{\varepsilon}) \\ &\leq |\tilde{d}_p|_1 G_1 + B_1 + 4\beta_{1p}(G_1)^{\varepsilon}, \end{aligned}$$

Hence,

$$\begin{aligned} D^+|E_p(t)|_1 &\leq 4\beta_p\varepsilon(G_1)^{\varepsilon-1}\Big(|\tilde{d}_p|_1 G_1 + B_1 + 4\beta_p(G_1)^{\varepsilon}\Big) \\ &= 4\beta_p|\tilde{d}_p|_1\varepsilon(G_1)^{\varepsilon} + 4B_1\beta_p\varepsilon(G_1)^{\varepsilon-1} + 16\beta_p^2\varepsilon(G_1)^{2\varepsilon-1} \\ &\triangleq H_1. \end{aligned}$$

For $t \in [t_s, t_{s+1})$, $|E_p(t)|_1 \leq H_1(t - t_s)$. When $t = t_{s+1}^-$,

$$|E_p(t_{s+1}^-)|_1 \leq H_1(t_{s+1} - t_s). \tag{22}$$

On the other hand, based on triggering condition (6),

$$|E_p(t_{s+1}^-)|_1 > \lambda_p(t), \quad t \in [t_s, t_{s+1}).$$

In light of Lemma 7, for any $t \in [t_s, t_{s+1})$,

$$\begin{aligned} \lambda_p(t) &= e^{\int_{t_s}^t(-\beth_p - \beta_p\lambda_p^{\varepsilon-1}(r))dr}\lambda_p(t_s) = e^{\int_{t_{s-1}}^t(-\beth_p - \beta_p\lambda_p^{\varepsilon-1}(r))dr}\lambda_p(t_{s-1}) \\ &= \cdots = e^{\int_0^t(-\beth_p - \beta_p\lambda_p^{\varepsilon-1}(r))dr}\lambda_p(0), \end{aligned}$$

thus,

$$|E_p(t_{s+1}^-)|_1 > e^{\int_0^t(-\beth_p - \beta_p\lambda_p^{\varepsilon-1}(r))dr}\lambda_p(0),$$

which combines (22),

$$\triangle s = t_{s+1} - t_s \geq \frac{e^{\int_0^t(-\beth_p - \beta_p\lambda_p^{\varepsilon-1}(r))dr}\lambda_p(0)}{H_1}.$$

Note that the event-triggering condition (6) is not satisfied after T_{st}, where T_{st} is the ST of QVFMNNs. In other words, we only need to verify that Zeno behavior does not occur for any $t \in (0, T_{st})$.

Firstly, when $\tilde{\kappa}_1 \leq 0$,

$$\triangle s > \frac{e^{\int_0^{T_1}(-\beth_p - \beta_p \lambda_p^{\varepsilon-1}(r))dr} \lambda_p(0)}{H_1} > 0.$$

Secondly, when $0 < \tilde{\kappa}_1 < \min\{nM_1, \tilde{\beta}_1\}$,

$$\triangle s > \frac{e^{\int_0^{T_2}(-\beth_p - \beta_p \lambda_p^{\varepsilon-1}(r))dr} \lambda_p(0)}{H_1} > 0.$$

Finally, when $0 < \tilde{\kappa}_1 < 2\sqrt{nM_1\tilde{\beta}_1}$,

$$\triangle s > \frac{e^{\int_0^{T_3}(-\beth_p - \beta_p \lambda_p^{\varepsilon-1}(r))dr} \lambda_p(0)}{H_1} > 0.$$

Therefore, under the event-triggered controller mechanism (5) and (6), systems (1) and (3) will not demonstrate the Zeno behavior. The proof is completed. □

3.2. PETS

The PETS of QVFMNNs (1) and (3) will be analyzed below. The controller based on the absolute value-like norm is characterized by

$$u_p(t) = -\frac{\hat{T}}{T_{1p}}[\alpha_p(t_{\bar{s}})](\gamma_p + \beta_p|\alpha_p(t_{\bar{s}})|_1^{\varepsilon}), \tag{23}$$

where T_{1p} is a positive preassigned time,

$$\hat{T} = \begin{cases} T_1, & \tilde{\kappa}_1 \leq 0, \\ T_2, & 0 < \tilde{\kappa}_1 < \min\{nM_1, \tilde{\beta}_1\}, \\ T_3, & 0 < \tilde{\kappa}_1 < 2\sqrt{nM_1\tilde{\beta}_1}, \ \varepsilon = 2. \end{cases}$$

The triggering condition is developed by

$$\begin{cases} t_{\bar{s}+1} = \inf\{t : t \geq t_{\bar{s}}, F_p(t) > 0\}, \\ F_p(t) = A_{1p} + |E_p(t)|_1 - \frac{\hat{T}}{T_{1p}}\gamma_p + \frac{\hat{T}}{T_{1p}}M_1 - \beth_p\lambda_p(t), \\ \dot{\lambda}_p(t) = -\beth_p\lambda_p(t) - \frac{\hat{T}}{T_{1p}}\beta_p\lambda_p^{\varepsilon}(t), \end{cases} \tag{24}$$

where $\lambda_p(t) > 0$,

$$E_p(t) = \frac{\hat{T}}{T_{1p}}[e_p(t_{\bar{s}})](\gamma_p + \beta_p|e_p(t_{\bar{s}})|_1^{\varepsilon}) - \frac{\hat{T}}{T_{1p}}[e_p(t)](\gamma_p + \beta_p|e_p(t)|_1^{\varepsilon}).$$

Theorem 3. *Based on Assumption 1, the PETS of systems (1) and (3) is realized within the preassigned time T_{1p} satisfying $0 < T_{1p} \leq \hat{T}$ under the control laws (23) and (24).*

Proof. Construct the following Lyapunov function

$$\hat{V}(t) = V_1(t) + V_3(t) = \sum_{p \in \mathbf{N}} |\alpha_p(t)|_1 + \sum_{p \in \mathbf{N}} \lambda_p(t).$$

Similar to the proof of Theorem 1,

$$\begin{aligned}
D^+V_1(t) \leq & \sum_{p \in \mathbf{N}} (\tilde{d}_p + \sum_{q \in \mathbf{N}} l_p \tilde{a}_{qp}) |\alpha_p(t)|_1 - \frac{\hat{T}}{T_{1p}} \sum_{p \in \mathbf{N}} \beta_p |\alpha_p(t)|_1^{\varepsilon} \\
& + \sum_{p \in \mathbf{N}} (A_{1p} + |E_p(t)|_1 - \frac{\hat{T}}{T_{1p}} \gamma_p) \\
\leq & \sum_{p \in \mathbf{N}} (\tilde{d}_p + \sum_{q \in \mathbf{N}} l_p \tilde{a}_{qp}) |\alpha_p(t)|_1 \\
& - \frac{\hat{T}}{T_{1p}} \sum_{p \in \mathbf{N}} \beta_p |\alpha_p(t)|_1^{\varepsilon} - \frac{\hat{T}}{T_{1p}} n M_1 \\
\leq & \tilde{\kappa}_1 \sum_{p \in \mathbf{N}} |\alpha_p(t)|_1 - \frac{\hat{T}}{T_{1p}} \sum_{p \in \mathbf{N}} \beta_p |\alpha_p(t)|_1^{\varepsilon} - \frac{\hat{T}}{T_{1p}} n M_1.
\end{aligned}$$

when $\tilde{\kappa}_1 \leq 0$,

$$D^+\hat{V}(t) \leq \frac{\hat{T}}{T_{1p}} \Big(- \tilde{\beta}_1 (V(t))^{\varepsilon} - n M_1 \Big).$$

In view of Lemma 2, the QVFMNNs (1) and (3) are preassigned-time synchronized within the time T_{1p}.

When $0 < \tilde{\kappa}_1 < \min\{n M_1, \tilde{\beta}_1\}$,

$$D^+\hat{V}(t) \leq \frac{\hat{T}}{T_{1p}} \Big(\tilde{\kappa}_1 V(t) - \tilde{\beta}_1 (V(t))^{\varepsilon} - n M_1 \Big).$$

The QVFMNNs (1) and (3) can realize PETS within the time T_{1p}. In particular, when $0 < \tilde{\kappa}_1 < 2\sqrt{n M_1 \tilde{\beta}_1}$, the PETS of QVFMNNs (1) and (3) is achieved within the time T_{1p}. □

The PETS of QVMNNs (14) and (15) will be analyzed below. To achieve this aim, the controller is proposed by

$$\hat{u}_p(t) = -\frac{\hat{\hat{T}}}{\hat{T}_{1p}} [\alpha_p(t_{\hat{\hat{s}}})] (\hat{\gamma}_p + \hat{\beta}_p |\alpha_p(t_{\hat{\hat{s}}})|_1^{\hat{\varepsilon}}), \;\; t \in [t_{\hat{\hat{s}}}, t_{\hat{\hat{s}}+1}), \tag{25}$$

where $\hat{T}_{1p}$ is a positive preassigned time,

$$\hat{\hat{T}} = \begin{cases} \hat{T}_1, \;\; \tilde{\kappa}_1 \leq 0, \\ \hat{T}_2, \;\; 0 < \tilde{\kappa}_1 < \min\{n\hat{M}_1, \tilde{\beta}_2\}, \\ \hat{T}_3, \;\; 0 < \tilde{\kappa}_1 < 2\sqrt{n\hat{M}_1 \tilde{\beta}_2}, \;\; \hat{\varepsilon} = 2. \end{cases}$$

The triggering condition is developed by

$$\begin{cases} t_{\hat{\hat{s}}+1} = \inf\{t : t \geq t_{\hat{\hat{s}}}, \hat{F}_p(t) > 0\}, \\ \hat{F}_p(t) = A_{2p} + |\hat{E}_p(t)|_1 - \dfrac{\hat{\hat{T}}}{\hat{T}_{1p}} \hat{\gamma}_p + \hat{M}_1 - \hat{\beth}_p \hat{\lambda}_p(t), \\ \dot{\hat{\lambda}}_p(t) = -\hat{\beth}_p \hat{\lambda}_p(t) - \dfrac{\hat{\hat{T}}}{\hat{T}_{1p}} \hat{\beta}_p \hat{\lambda}_p^{\hat{\varepsilon}}(t), \end{cases} \tag{26}$$

where $\hat{\lambda}_p(t) > 0$,

$$\hat{E}_p(t) = \frac{\hat{\hat{T}}}{\hat{T}_{1p}}[\alpha_p(t_{\hat{\xi}})](\hat{\gamma}_p + \hat{\beta}_p|\alpha_p(t_{\hat{\xi}})|_1^{\hat{\varepsilon}}) - \frac{\hat{\hat{T}}}{\hat{T}_{1p}}[\alpha_p(t)](\hat{\gamma}_p + \hat{\beta}_p|\alpha_p(t)|_1^{\hat{\varepsilon}}).$$

Corollary 3. *Based on Assumption 1, the PETS of networks (14) and (15) is realized within the preassigned time $\hat{T}_{1p}$ satisfying $0 < \hat{T}_{1p} \leq \hat{\hat{T}}$ under the control laws (25) and (26).*

In order to achieve the PETS of QVFNNs (18) and (19), the controller is designed by

$$\check{u}_p(t) = -\frac{\check{\check{T}}}{\check{T}_{1p}}[\alpha_p(t_{\check{\xi}})](\check{\gamma}_p + \check{\beta}_p|\alpha_p(t_{\check{\xi}})|_1^{\check{\varepsilon}}), \ \ t \in [t_{\check{\xi}}, t_{\check{\xi}+1}), \tag{27}$$

where $\check{T}_{1p}$ is a positive preassigned time,

$$\check{\check{T}} = \begin{cases} \check{T}_1, \ \ \tilde{\kappa}_1 \leq 0, \\ \check{T}_2, \ \ 0 < \tilde{\kappa}_1 < \min\{n\check{M}_1, \tilde{\beta}_3\}, \\ \check{T}_3, \ \ 0 < \tilde{\kappa}_1 < 2\sqrt{n\check{M}_1\tilde{\beta}_3}, \ \ \check{\varepsilon} = 2. \end{cases}$$

The triggering condition is developed by

$$\begin{cases} t_{\check{\xi}+1} = \inf\{t : t \geq t_{\check{\xi}}, \check{F}_p(t) > 0\}, \\ \check{F}_p(t) = A_{3p} + |\check{E}_p(t)|_1 - \frac{\check{\check{T}}}{\check{T}_{1p}}\check{\gamma}_p + \check{M}_1 - \check{\beth}_p\check{\lambda}_p(t), \\ \dot{\check{\lambda}}_p(t) = -\check{\beth}_p\check{\lambda}_p(t) - \frac{\check{\check{T}}}{\check{T}_{1p}}\check{\beta}_p\check{\lambda}_p^{\check{\varepsilon}}(t), \end{cases} \tag{28}$$

where $\check{\lambda}_p(t) > 0$, and the measure error $\check{E}_p(t)$ is defined by

$$\check{E}_p(t) = \frac{\check{\check{T}}}{\check{T}_{1p}}[\alpha_p(t_{\check{\xi}})](\check{\gamma}_p + \check{\beta}_p|\alpha_p(t_{\check{\xi}})|_1^{\check{\varepsilon}}) - \frac{\check{\check{T}}}{\check{T}_{1p}}[\alpha_p(t)](\check{\gamma}_p + \check{\beta}_p|\alpha_p(t)|_1^{\check{\varepsilon}}).$$

Corollary 4. *Based on Assumption 1, the networks (18) and (19) are PETS within the preassigned time $\check{T}_{1p}$ satisfying $0 < \check{T}_{1p} \leq \check{\check{T}}$ under the control laws (27) and (28).*

Remark 7. *Specifically, when the QVFMNNs (1) and (3) are simplified into real-valued [4] or complex-valued [29] NN models, the control strategies outlined in this paper can also be adapted for use with real or complex-variable control laws. Additionally, the synchronization conditions established herein are applicable to systems with either real or complex variables.*

Remark 8. *In [22], the authors addressed the challenges of higher-dimensional data by proposing a criterion for achieving FITS in octonion-valued neural networks. Building upon the insight gained from these studies, our forthcoming research aims to explore the FITS and PETS of octonion-valued neural networks by adaptive event-triggered control.*

Remark 9. *Take Theorem 1 as an example, the following steps (Table 1) can be used to achieve FITS of (1) and (3).*

Table 1. FITS control algorithm.

Parameter Selection Steps in Theorem 1.
Step 1: the value of $\widetilde{k}_1$ is calculated by using the parameters $A_{1p}, A_{2p}, A_{3p}, l_p^1$ and $\widetilde{l}_p^1$. **Step 2:** choose control parameters $\gamma_p, \beta_p, \gimel_p, M_1$ and ε in the controller (5) and (6). **Step 3:** estimate the setting time $T_1(T_2, T_3)$. **Step 4:** draw the simulation result of FITS.

4. Numerical Simulations

In this section, three numerical examples are presented to verify the above theoretical results.

Example 1. *Consider the following QVFMNN with two neurons*

$$\begin{aligned}\dot{w}_p(t) = &-d_p(w_p(t))w_p(t) + \sum_{q=1,2} a_{pq}(w_p(t))f_q(w_q(t)) \\ &+ \sum_{q=1,2} b_{pq}(w_p(t))g_q(w_q(m_{pq}(t))) \\ &+ \bigvee_{q=1,2} \theta_{pq}g_q(w_q(m_{pq}(t))) + \sum_{q=1,2} c_{pq}\eta_q \\ &+ \bigwedge_{q=1,2} \sigma_{pq}g_q(w_q(m_{pq}(t))) + \bigvee_{q=1,2} \phi_{pq}\eta_q \\ &+ \bigwedge_{q=1,2} \psi_{pq}\eta_q + \xi_p, \quad p = 1,2,\end{aligned} \tag{29}$$

where $w_p(t) \in \mathbb{Q}$, $f_q(x) = 0.82\tanh(x^R) + i0.82\sin(x^I) + j0.82\tanh(x^J) + k0.82\sin(x^K)$, $g_q(x) = 0.88\sin(x^R) + i0.88\sin(x^I) + j0.88\sin(x^J) + k0.88\sin(x^K)$, $m_{pq}(t) = t - \frac{e^t}{1+e^t}$, $\theta_{11} = 0.5$, $\theta_{12} = 0.4$, $\theta_{21} = 0.2$, $\theta_{22} = 0.6$, $\sigma_{11} = 0.2$, $\sigma_{12} = 0.3$, $\sigma_{21} = 0.7$, $\sigma_{22} = 0.5$, $\eta_1 = 1$, $\eta_2 = 0.8$, $\xi_1 = \xi_2 = 0$, *and*

$$(\phi_{pq})_{2\times 2} = \begin{pmatrix} 0.8 - 2.0i + 0.8j - 1.4k & 0.6 + 0.8i + 0.6j + 0.4k \\ 1.4 + 0.6i + 1.6j - 1.8k & -1.3 - 1.5i + 0.9j - 0.5k \end{pmatrix},$$

$$(\psi_{pq})_{2\times 2} = \begin{pmatrix} 0.6 - 1.0i + 1.0j - 2.4k & 1.3 - 1.6i + 1.3j - 1.8k \\ 0.8 - 1.2i + 1.2j - 1.3k & 1.1 - 0.6i + 1.4j - 0.6k \end{pmatrix},$$

and memristive weights are given as

$$d_1(x_1(t)) = \begin{cases} -2.10 - 2.20 - 2.50j - 2.20k, |x_1(t)|_1 \le 0.90, \\ -1.16 - 2.20i - 1.56j - 1.61k, |x_1(t)|_1 > 0.90, \end{cases}$$

$$d_2(x_2(t)) = \begin{cases} -1.40 - 1.50i - 1.80j - 2.20k, |x_2(t)|_1 \le 0.90, \\ -1.56 - 4.00i - 1.70j - 2.20k, |x_2(t)|_1 > 0.90, \end{cases}$$

$$a_{11}(x_1(t)) = \begin{cases} -1.80 - 1.50i - 0.80j - 1.80k, |x_1(t)|_1 \le 0.90, \\ 2.00 - 0.80i + 0.40j - 0.70k, |x_1(t)|_1 > 0.90, \end{cases}$$

$$a_{12}(x_1(t)) = \begin{cases} 0.60 + 0.90i + 1.30j - 1.30k, |x_1(t)|_1 \le 0.90, \\ -0.80 + 3.50i - 0.50j - 0.90k, |x_1(t)|_1 > 0.90, \end{cases}$$

$$a_{21}(x_2(t)) = \begin{cases} -1.50 - 1.66i - 1.50j - 1.36k, |x_2(t)|_1 \le 0.90, \\ -0.60 + 0.56i - 0.80j - 0.60k, |x_2(t)|_1 > 0.90, \end{cases}$$

$$a_{22}(x_2(t)) = \begin{cases} -1.00 - 0.40i - 1.40j + 0.50k, |x_2(t)|_1 \leq 0.90, \\ 1.50 - 2.00i - 0.35j + 0.65k, |x_2(t)|_1 > 0.90, \end{cases}$$

$$b_{11}(x_1(t)) = \begin{cases} -1.20 + 1.20i - 1.60j - 0.50k, |x_1(t)|_1 \leq 0.90, \\ -1.85 + 0.50i - 1.40j + 0.50k, |x_1(t)|_1 > 0.90, \end{cases}$$

$$b_{12}(x_1(t)) = \begin{cases} -1.30 - 0.50i - 1.50j + 0.25k, |x_1(t)|_1 \leq 0.90, \\ -0.20 + 2.80i - 1.00j + 0.69k, |x_1(t)|_1 > 0.90, \end{cases}$$

$$b_{21}(x_2(t)) = \begin{cases} -1.90 - 2.30i - 1.60j - 1.45k, |x_2(t)|_1 \leq 0.90, \\ -1.20 - 0.80i - 1.80j + 0.80k, |x_2(t)|_1 > 0.90, \end{cases}$$

$$b_{22}(x_2(t)) = \begin{cases} -0.10 - 0.90i + 1.20j - 0.50k, |x_2(t)|_1 \leq 0.90, \\ -0.20 - 1.00i - 0.80j - 0.55k, |x_2(t)|_1 > 0.90. \end{cases}$$

Set $x_1(s) = -1.50 - 1.00i - 1.50j - 1.60k$ and $x_2(s) = -1.80 + 1.50i - 2.00j + 1.50k$ as the initial conditions of (29), in which $s \in [-0.5, 0)$. Then, the chaotic behaviors of system (29) is shown in Figures 2–5.

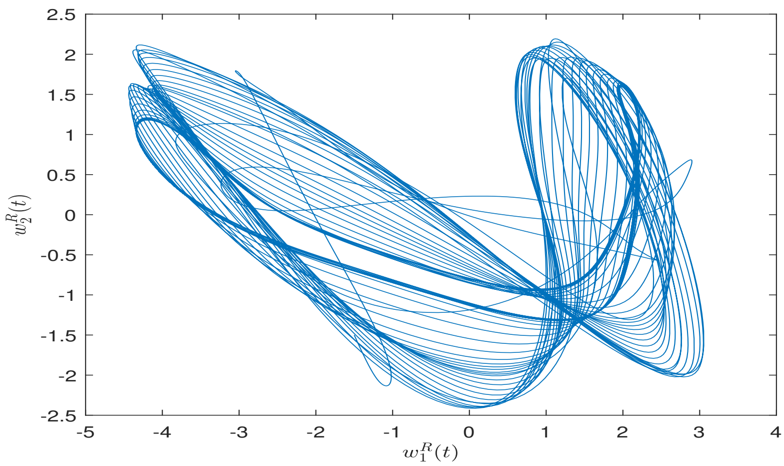

Figure 2. Chaotic behaviors of $x_1^R(t)$ and $x_2^R(t)$.

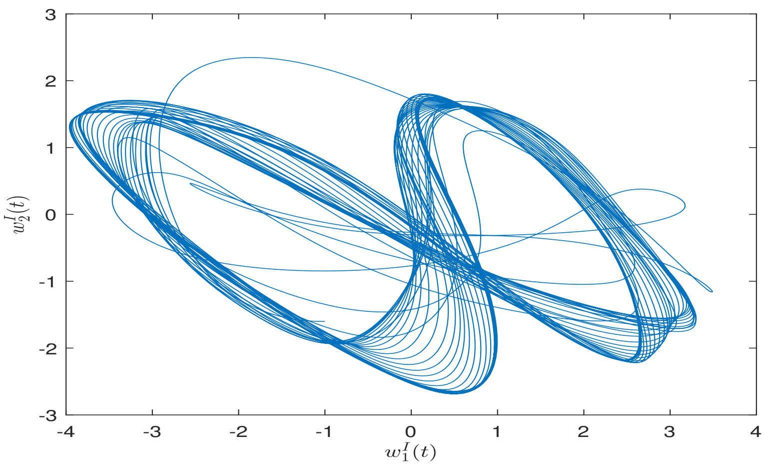

Figure 3. Chaotic behaviors of $x_1^I(t)$ and $x_2^I(t)$.

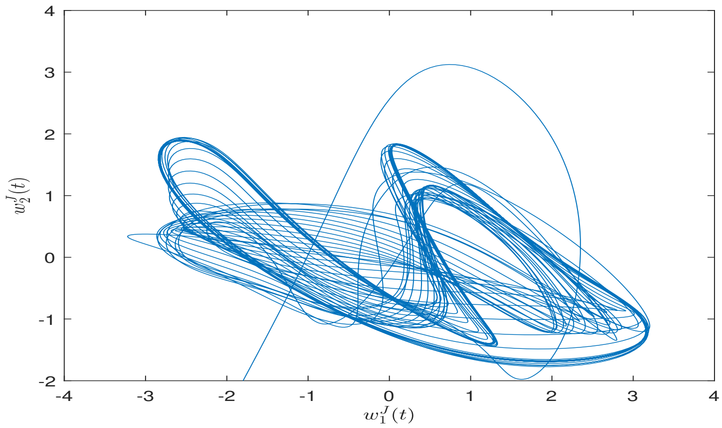

Figure 4. Chaotic behaviors of $x_1^J(t)$ and $x_2^J(t)$.

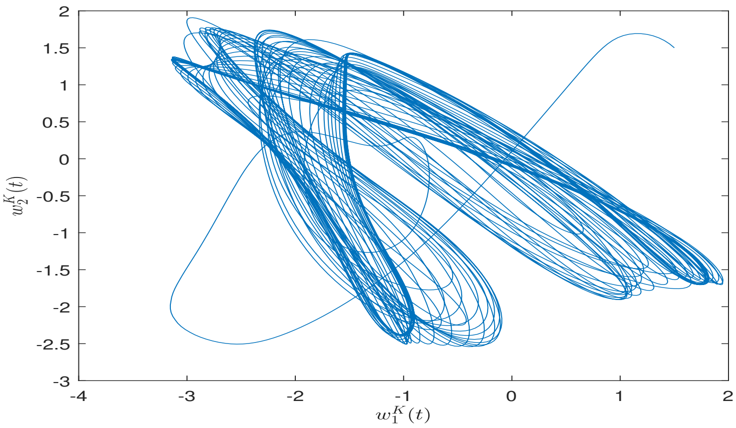

Figure 5. Chaotic behaviors of $x_1^K(t)$ and $x_2^K(t)$.

The response system of system (31) is described by

$$\begin{aligned}\dot{\delta}_p(t) = &-d_p(\delta_p(t))\delta_p(t) + \sum_{q=1,2} a_{pq}(\delta_p(t))f_q(\delta_q(t)) \\ &+ \sum_{q=1,2} b_{pq}(\delta_p(t))g_q(\delta_q(m_{pq}(t))) \\ &+ \bigvee_{q=1,2} \theta_{pq}g_q(\delta_q(m_{pq}(t))) + \sum_{q=1,2} c_{pq}\eta_q \\ &+ \bigwedge_{q=1,2} \sigma_{pq}g_q(\delta_q(m_{pq}(t))) + \bigvee_{q=1,2} \phi_{pq}\eta_q \\ &+ \bigwedge_{q=1,2} \psi_{pq}\eta_q + \xi_p + u_p(t), \quad p = 1,2.\end{aligned} \tag{30}$$

Set $\delta_1(s) = 1.90 - 1.80i - 1.30j + 1.60k$ and $\delta_2(s) = 1.10 - 1.50i - 2.00j - 1.60k$ as the initial conditions of (32), in which $s \in [-0.5, 0)$.

Firstly, to verify the FITS results of (29) and (30) based on event-triggered control mechanism (5) and (6), select $\gamma_1 = 18$, $\gamma_2 = 14$, $\beta_1 = 5$, $\beta_2 = 6$, $\varepsilon = 1.2$, $M_1 = 0.5$, $\daleth_1 = 2$, $\daleth_2 = 1.2$, $\lambda_1(0) = 20$, and $\lambda_2(0) = 15$. By means of Theorems 1 and 2, the QVFMNNs (29) and (30) can achieve FITS, and the settling time is estimated by $T_1 = 1.7250$. The synchronization results are shown in Figures 6–8.

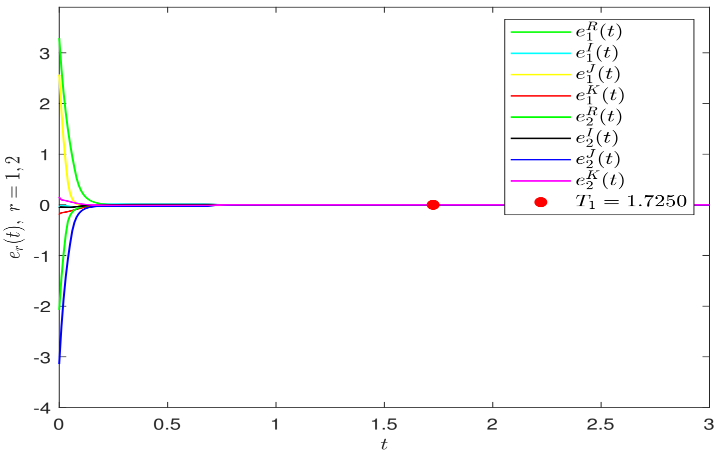

Figure 6. Synchronization errors of QVFMNNs (31) and (32) under controller (5).

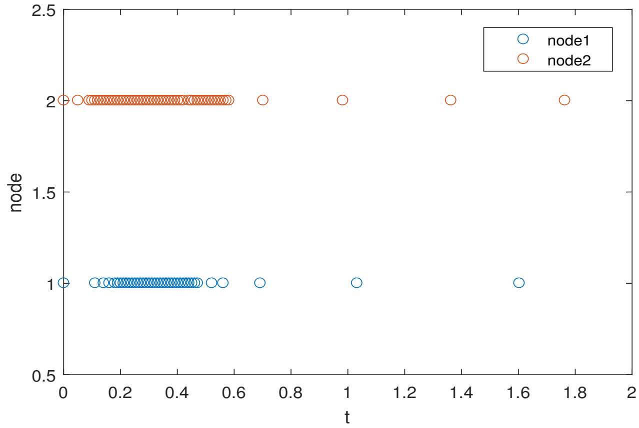

Figure 7. Triggering instants of each neuron.

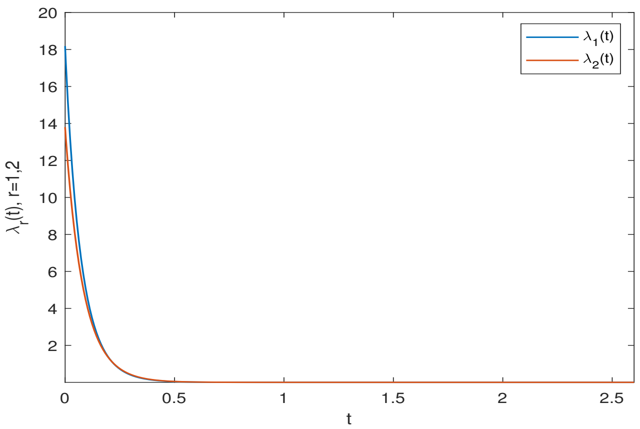

Figure 8. The dynamic evolution of $\lambda_r(t)$.

In addition, choose $T_{1p} = 1.0$ in (23). The PETS of QVFMNNs (31) and (32) can be realized within the preassigned time T_{1p} according to Theorem 3, which is demonstrated in Figures 9 and 10.

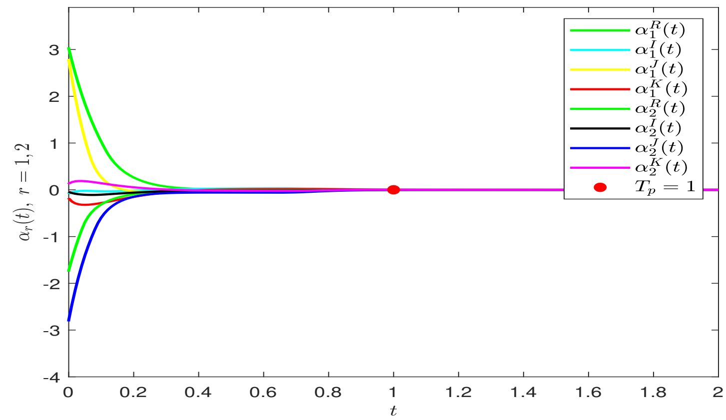

Figure 9. Synchronization errors of QVFMNNs (31) and (32) under controller (23).

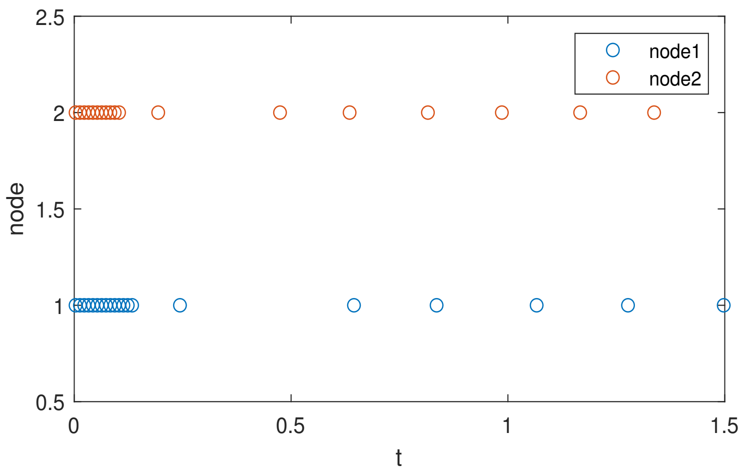

Figure 10. Triggering instants of each neuron.

Remark 10. *In Figure 6, the trajectories of the FITS errors are shown, which are convergent within* $T_1 = 1.7250$ *in Theorem 1. The exclusion of Zeno behavior is demonstrated as shown in Figure 7. Similarly, Figures 8 and 9 validate the prescribed-time synchronization results mentioned in Theorem 3. In addition, with identical parameter settings, the estimated ST is 2.3513. Clearly, the settling time estimation presented in this study is more precise. The relevant result is displayed in Table 2.*

Table 2. Comparison of settling-time estimation.

$(\gamma_1, \gamma_2, \beta_1, \beta_2, \epsilon)$ = (18, 14, 5, 6, 1.2)		
	Refs. [22,24,33]	Example 1
estimation of settling time	2.3513	1.7250

Example 2. *Consider the following QVMNN with two neurons*

$$\begin{aligned}\dot{w}_p(t) = -d_p(w_p(t))w_p(t) + \sum_{q=1,2} a_{pq}(w_p(t))f_q(w_q(t)) \\ + \sum_{q=1,2} b_{pq}(w_p(t))g_q(w_q(m_{pq}(t))) + \xi_p, \quad p = 1,2,\end{aligned} \tag{31}$$

where $w_p(t) \in \mathbb{Q}$, $f_q(x) = 0.82\tanh(x^R) + i0.82\sin(x^I) + j0.82\tanh(x^J) + k0.82\sin(x^K)$, $g_q(x) = 0.88\sin(x^R) + i0.88\sin(x^I) + j0.88\sin(x^J) + k0.88\sin(x^K)$, $m_{pq}(t) = t - \frac{e^t}{1+e^t}$, $\xi_1 = \xi_2 = 0$, *and memristive weights are given as*

$$d_1(x_1(t)) = \begin{cases} -2.10 - 2.20 - 2.50j - 2.20k, |x_1(t)|_1 \le 0.90, \\ -1.10 - 2.20i - 1.50j - 1.61k, |x_1(t)|_1 > 0.90, \end{cases}$$

$$d_2(x_2(t)) = \begin{cases} -1.30 - 1.50i - 1.80j - 2.20k, |x_2(t)|_1 \le 0.90, \\ -1.50 - 4.00i - 1.50j - 2.20k, |x_2(t)|_1 > 0.90, \end{cases}$$

$$a_{11}(x_1(t)) = \begin{cases} -1.80 - 1.50i - 0.80j - 1.80k, |x_1(t)|_1 \le 0.90, \\ 2.00 - 0.80i + 1.40j - 0.70k, |x_1(t)|_1 > 0.90, \end{cases}$$

$$a_{12}(x_1(t)) = \begin{cases} 0.50 + 0.90i + 1.50j - 1.30k, |x_1(t)|_1 \le 0.90, \\ -0.70 + 3.50i - 0.80j - 0.90k, |x_1(t)|_1 > 0.90, \end{cases}$$

$$a_{21}(x_2(t)) = \begin{cases} 1.50 - 1.66i - 1.50j - 2.30k, |x_2(t)|_1 \le 0.90, \\ -0.60 + 0.50i - 1.80j - 0.60k, |x_2(t)|_1 > 0.90, \end{cases}$$

$$a_{22}(x_2(t)) = \begin{cases} -2.00 - 1.40i - 1.40j + 0.50k, |x_2(t)|_1 \le 0.90, \\ 1.50 - 2.00i - 1.30j + 0.60k, |x_2(t)|_1 > 0.90, \end{cases}$$

$$b_{11}(x_1(t)) = \begin{cases} -1.20 + 1.20i - 1.60j - 0.50k, |x_1(t)|_1 \le 0.90, \\ -1.80 + 0.50i - 1.40j + 0.50k, |x_1(t)|_1 > 0.90, \end{cases}$$

$$b_{12}(x_1(t)) = \begin{cases} -1.30 - 1.50i - 1.50j + 0.25k, |x_1(t)|_1 \le 0.90, \\ -0.20 + 2.80i - 1.20j + 0.40k, |x_1(t)|_1 > 0.90, \end{cases}$$

$$b_{21}(x_2(t)) = \begin{cases} -1.90 - 2.30i - 1.60j - 1.45k, |x_2(t)|_1 \le 0.90, \\ -1.20 - 0.80i - 1.80j + 0.80k, |x_2(t)|_1 > 0.90, \end{cases}$$

$$b_{22}(x_2(t)) = \begin{cases} -0.15 - 0.90i + 1.20j - 0.50k, |x_2(t)|_1 \le 0.90, \\ -1.20 - 1.00i - 1.80j - 0.50k, |x_2(t)|_1 > 0.90. \end{cases}$$

Set $x_1(s) = -1.80 - 1.20i - 0.50j - 1.60k$ and $x_2(s) = -0.80 + 1.20i - 2.00j + 1.50k$ as the initial conditions of (31), in which $s \in [-0.5, 0)$. Then, the chaotic behaviors of system (31) is shown in Figures 11–14.

The response system of system (31) is described by

$$\begin{aligned} \dot{\delta}_p(t) = &-d_p(\delta_p(t))\delta_p(t) + \sum_{q=1,2} a_{pq}(\delta_p(t)) f_q(\delta_q(t)) \\ &+ \sum_{q=1,2} b_{pq}(\delta_p(t)) g_q(\delta_q(m_{pq}(t))) + \xi_p + u_p(t), \quad p = 1, 2. \end{aligned} \tag{32}$$

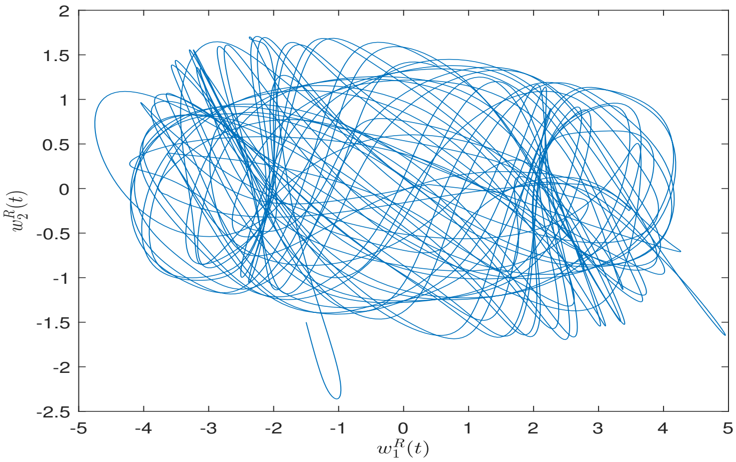

Figure 11. Chaotic behaviors of $x_1^R(t)$ and $x_2^R(t)$.

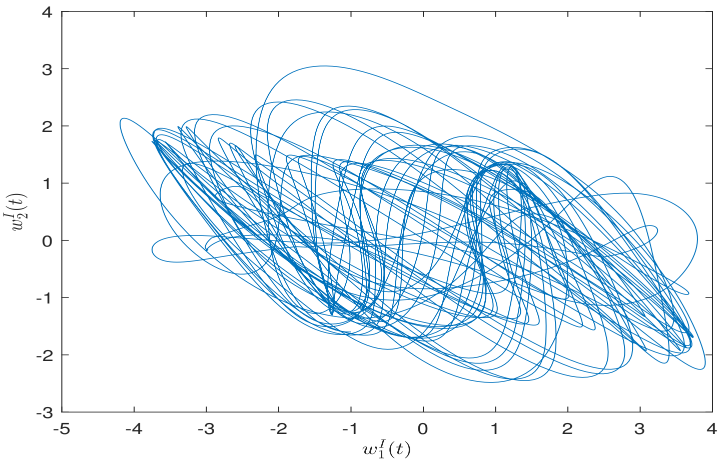

Figure 12. Chaotic behaviors of $x_1^I(t)$ and $x_2^I(t)$.

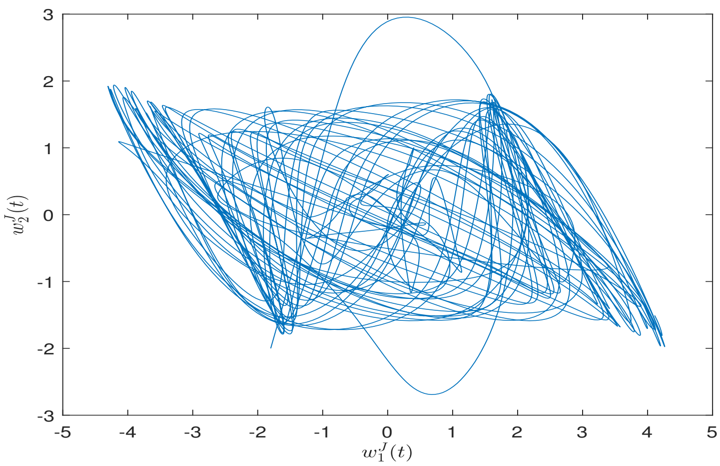

Figure 13. Chaotic behaviors of $x_1^J(t)$ and $x_2^J(t)$.

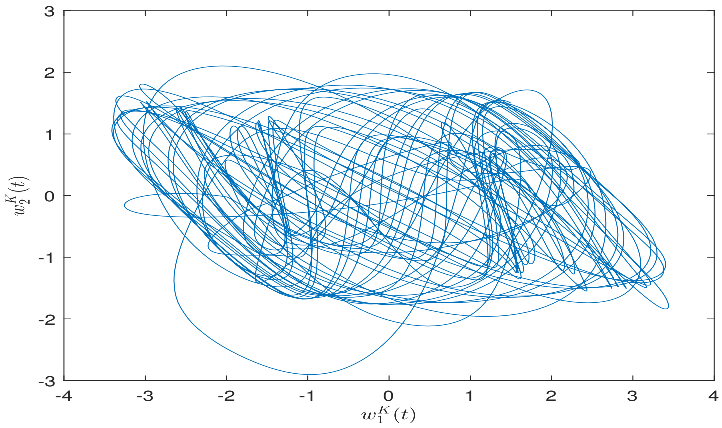

Figure 14. Chaotic behaviors of $x_1^K(t)$ and $x_2^K(t)$.

Set $\delta_1(s) = 1.90 - 2.80i - 2.30j + 1.60k$ and $\delta_2(s) = 1.00 - 2.50i - 2.00j - 2.60k$ as the initial conditions of (32), in which $s \in [-0.5, 0)$.

Firstly, the FITS results of (31) and (32) based on event-triggered control mechanism (16) and (17) are verified, select $\hat{\gamma}_1 = 10$, $\hat{\gamma}_2 = 12$, $\hat{\beta}_1 = 4$, $\hat{\beta}_2 = 5$, $\hat{\varepsilon} = 1.3$, $\hat{M}_1 = 0.6$, $\hat{\gimel}_1 = 3$, $\hat{\gimel}_2 = 2$, $\hat{\lambda}_1(0) = 12$, and $\hat{\lambda}_2(0) = 14$. Based on Corollary 1, the QVMNNs (31) and (32) can achieve FITS, and the settling time is estimated by $\hat{T}_1 = 1.4634$. The synchronization results are shown in Figures 15–17.

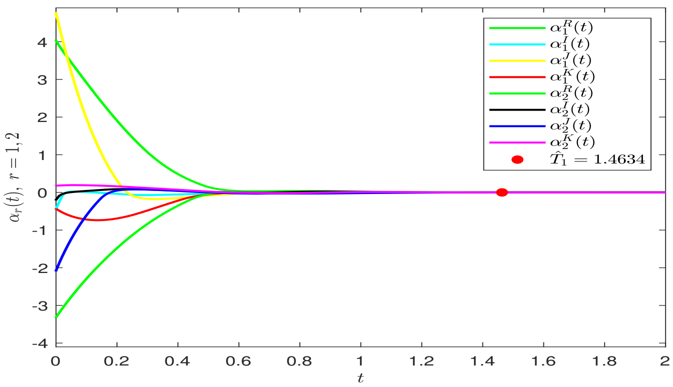

Figure 15. Synchronization errors of QVFMNNs (31) and (32) under controller (16).

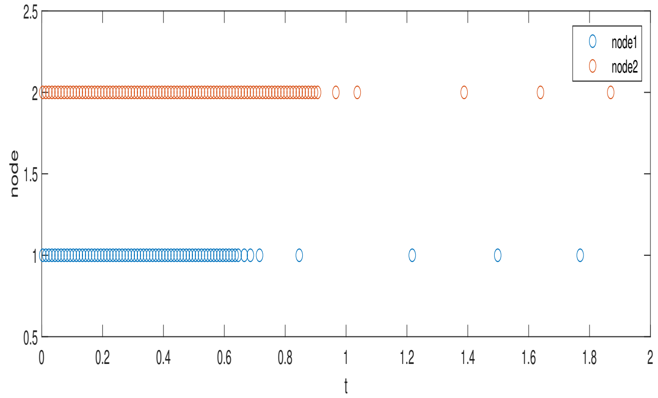

Figure 16. Triggering instants of each neuron.

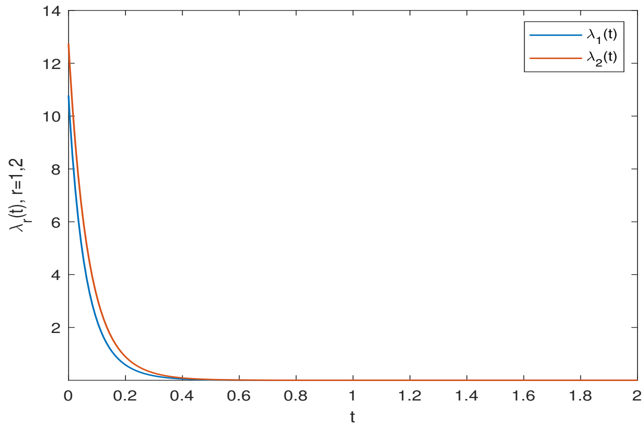

Figure 17. The dynamic evolution of $\lambda_r(t)$.

Furthermore, choose $\hat{T}_{1p} = 1.2$ in (25). The PETS of QVMNNs (31) and (32) can be realized within the preassigned time $\hat{T}_{1p} = 1.2$ according to Corollary 3, which are demonstrated in Figures 18 and 19.

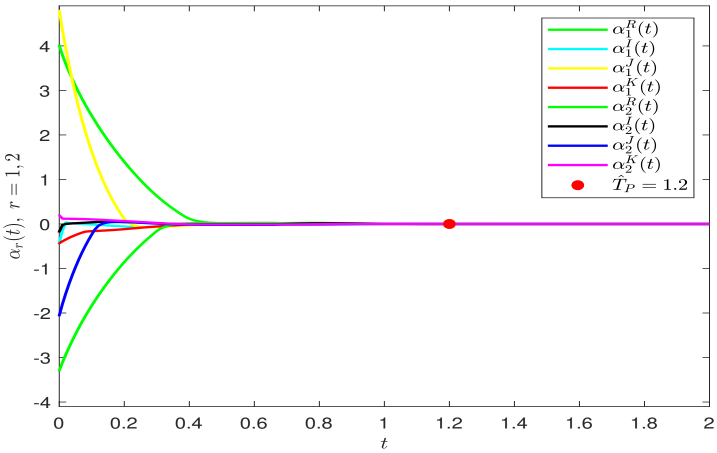

Figure 18. Synchronization errors of QVFMNNs (31) and (32) under controller (25).

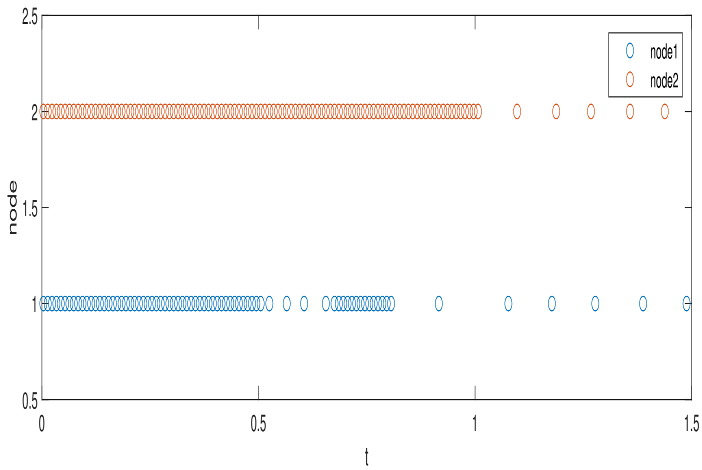

Figure 19. Triggering instants of each neuron.

5. Conclusions

In this paper, under the framework of a direct analysis approach, the synchronization of delayed QVNNs including fuzzy term and memristive were investigated in a fixed time and preassigned time, respectively. Firstly, unlike the existing quaternion-valued fuzzy rules [28,40–42], a new fuzzy rule was proposed in the quaternion field, and the some important properties were established. Furthermore, several dynamic event-triggering protocols were designed to ensure FITS and PETS, and the established synchronization criteria were more concise than the existing separation results. Lastly, the effectiveness and applicability of the main results of this paper were verified by two numerical examples.

Note that the finite-time and FITS of the second-order NNs have been explored by means of reduced-order variable substitution techniques. Nevertheless, there seems to be few related works to discussed the FITS and PETS of QVMNNs with delay by using direct analytical method and a dynamic event-triggering approach. The challenging problem will be addressed in our future work.

Author Contributions: Methodology, S.J.; Software, H.J.; Investigation, C.H.; Writing—original draft, S.J. All authors have read and agreed to the published version of the manuscript.

Funding: This work was supported jointly by National Natural Science Foundation of China (62163035), by the Key Project of Natural Science Foundation of Xinjiang (2021D01D10), by the Special Project for Local Science and Technology Development Guided by the Central Government (ZYYD2022A05), by Tianshan Talent Program (2022TSYCLJ0004), by Excellent Doctor Innovation program of Xinjiang University (XJUBSCX-201929).

Data Availability Statement: Data are contained within the article.

Conflicts of Interest: The authors declare no conflicts of interest.

Abbreviations

$\mathbb{R}$	$\mathbb{R} = (-\infty, +\infty)$
$\mathbb{Q}$	The quaternion set
$\mathbb{R}^n$	The n-dimensional real number vector set
$\mathbb{Q}^n$	The n-dimensional quaternion number vector set
$\mathbf{N}$	$\mathbf{N} = \{1, 2, \cdots n\}$
$\varkappa$	$\varkappa = \{R, I, J, K\}$
$\lvert\mathbf{w}\rvert_1$	$\lvert\mathbf{w}\rvert_1 = \lvert\mathbf{w}^R\rvert + \lvert\mathbf{w}^I\rvert + \lvert\mathbf{w}^J\rvert + \lvert\mathbf{w}^K\rvert$, for any $\mathbf{w} = \mathbf{w}^R + i\mathbf{w}^I + j\mathbf{w}^J + k\mathbf{w}^K \in \mathbb{Q}$
$\mathbf{a}^{\varkappa -}(\mathbf{w})$	The left limit of discontinuous function $\mathbf{a}(\cdot) : \mathbb{Q} \to \mathbb{Q}$ at point $\mathbf{w} \in \mathbb{Q}$
$\mathbf{a}^{\varkappa +}(\mathbf{w})$	The right limit of discontinuous function $\mathbf{a}(\cdot) : \mathbb{Q} \to \mathbb{Q}$ at point $\mathbf{w} \in \mathbb{Q}$
$\grave{\mathbf{a}}^{\varkappa}(\mathbf{w})$	The minimum of $\mathbf{a}^{\varkappa -}(\mathbf{w})$
$\acute{\mathbf{a}}^{\varkappa}(\mathbf{w})$	The maximum of $\mathbf{a}^{\varkappa +}(\mathbf{w})$
$\bar{co}[\mathbf{a}(\mathbf{w})]$	$\bar{co}[\mathbf{a}(\mathbf{w})] = \bar{co}[\mathbf{a}^R(\mathbf{w})] + \bar{co}[\mathbf{a}^I(\mathbf{w})]i + \bar{co}[\mathbf{a}^J(\mathbf{w})]j$ $+\bar{co}[\mathbf{a}^K(\mathbf{w})]k$, in which $\bar{co}[\mathbf{a}^R(\mathbf{w})] = [\acute{\mathbf{a}}^R(\mathbf{w}), \grave{\mathbf{a}}^R(\mathbf{w})]$ $\bar{co}[\mathbf{a}^I(\mathbf{w})] = [\acute{\mathbf{a}}^I(\mathbf{w}), \grave{\mathbf{a}}^I(\mathbf{w})]$, $\bar{co}[\mathbf{a}^J(\mathbf{w})] = [\acute{\mathbf{a}}^J(\mathbf{w}), \grave{\mathbf{a}}^J(\mathbf{w})]$, $\bar{co}[\mathbf{a}^K(\mathbf{w})] = [\acute{\mathbf{a}}^K(\mathbf{w}), \grave{\mathbf{a}}^K(\mathbf{w})]$

References

1. Liu, F.; Meng, W.; Lu, R. Anti-synchronization of discrete-time fuzzy memristive neural networks via impulse sampled-data communication. *IEEE Trans. Cybern.* **2023**, *53*, 4122–4133. [CrossRef] [PubMed]
2. Wei, H.; Li, R. Exponential synchronization control of reaction-diffusion fuzzy memristive neural networks: Hardy-Poincare inequality. *IEEE Trans. Neural Netw. Learn. Syst.* **2023**, *online ahead of print*. [CrossRef]
3. Gong, S.; Guo, Z.; Wen, S. Finite-time synchronization of T-S fuzzy memristive neural networks with time delay. *Fuzzy Sets Syst.* **2022**, *459*, 67–81. [CrossRef]
4. Wang, L.; Li, H.; Hu, C.; Hu, J.; Wang, Q. Synchronization and settling-time estimation of fuzzy memristive neural networks with time-varying delays: Fixed-time and preassigned-time control. *Fuzzy Sets Syst.* **2023**, *470*, 108654. [CrossRef]
5. Davila-Meza, E.; Bayro-Corrochano, E. Quaternion and split quaternion neural networks for low-light color image enhancement. *IEEE Access* **2023**, *11*, 108257–108280. [CrossRef]
6. Frants, V.; Agaian, S.; Panetta, K. QSAM-Net: Rain streak removal by quaternion neural network with self-attention module. *IEEE Trans. Multimed.* **2023**, *26*, 789–798. [CrossRef]
7. Ni, H.; Xie, S.; Xu, P.; Fang, X.; Sun, W.; Fang, R. QMGR-Net: Quaternion multi-graph reasoning network for 3D hand pose estimation. *Int. J. Mach. Learn. Cybern.* **2023**, *14*, 4029–4045. [CrossRef]
8. Shi, Y.; Chen, X.; Zhu, P. Dissipativity for a class of quaternion-valued memristor-based neutral-type neural networks with time-varying delays. *Math. Methods Appl. Sci.* **2023**, *46*, 18166–18194. [CrossRef]
9. Aouiti, C.; Touati, F. Global dissipativity of quaternion-valued fuzzy cellular fractional-order neural networks with time delays. *Neural Process. Lett.* **2022**, *55*, 481–503. [CrossRef]
10. Chen, Y.; Xue, Y.; Yang, X.; Zhang, X. A direct analysis method to Lagrangian global exponential stability for quaternion memristive neural networks with mixed delays. *Appl. Math. Comput.* **2022**, *439*, 127633. [CrossRef]
11. Liu, Y.; Zhang, D.; Lou, J.; Lu, J.; Cao, J. Stability analysis of quaternion-valued neural networks: Decomposition and direct approaches. *IEEE Trans. Neural Netw. Learn. Syst.* **2018**, *29*, 4201–4211. [CrossRef]
12. Liu, Y.; Zheng, Y.; Lu, J.; Cao, J.; Rutkowski, L. Constrained quaternion-variable convex optimization: A quaternion-valued recurrent neural network approach. *IEEE Trans. Neural Netw. Learn. Syst.* **2020**, *31*, 1022–1035. [CrossRef]
13. Peng, T.; Wu, Y.; Tu, Z.; Alofi, A.; Lu, J. Fixed-time and prescribed-time synchronization of quaternion-valued neural networks: A control strategy involving Lyapunov functions. *Neural Netw.* **2023**, *160*, 108–121. [CrossRef] [PubMed]
14. Shang, W.; Zhang, W.; Chen, D.; Cao, J. New criteria of finite time synchronization of fractional-order quaternion-valued neural networks with time delay. *Appl. Math. Comput.* **2022**, *436*, 127484. [CrossRef]
15. Zhang, L.; Wei, R.; Cao, J.; Ding, X. Synchronization control of quaternion-valued inertial memristor-based neural networks via adaptive method. *Math. Methods Appl. Sci.* **2024**, *47*, 581–599. [CrossRef]
16. Zhang, T.; Jian, J. Quantized intermittent control tactics for exponential synchronization of quaternion-valued memristive delayed neural networks. *ISA Trans.* **2021**, *126*, 288–299. [CrossRef] [PubMed]
17. Lin, D.; Chen, X.; Yu, G.; Li, Z.; Xia, Y. Global exponential synchronization via nonlinear feedback control for delayed inertial memristor-based quaternion-valued neural networks with impulses. *Appl. Math. Comput.* **2021**, *401*, 126093. [CrossRef]
18. Aouiti, C.; Jallouli, H. New feedback control techniques of quaternion fuzzy neuralnetworks with time-varying delay. *Int. J. Robust Nonlinear Control* **2021**, *31*, 2783–2809. [CrossRef]
19. Wang, P.; Li, X.; Wang, N.; Li, Y.; Shi, K.; Lu, J. Almost periodic synchronization of quaternion-valued fuzzy cellular neural networks with leakage delays. *Fuzzy Sets Syst.* **2021**, *426*, 46–65. [CrossRef]
20. Narayanan, G.; Ali, M.; Alam, M.; Rajchakit, G.; Boonsatit, N.; Kumar, P.; Hammachukiattikul, P. Adaptive fuzzy feedback controller design for finite-time mittag-leffler synchronization of fractional-order quaternion-valued reaction-diffusion fuzzy molecular modeling of delayed neural networks. *IEEE Access* **2021**, *9*, 130862–130883. [CrossRef]
21. Tang, Q.; Qu, S.; Zheng, W.; Du, X.; Tu, Z. New fixed-time stability criterion and fixed-time synchronization of neural networks via non-chattering control. *Neural Comput. Appl.* **2022**, *35*, 6029–6041. [CrossRef]
22. Chouhan, S.; Kumar, U.; Das, S.; Cao, J. Fixed time synchronization of octonion valued neural networks with time varying delays. *Eng. Appl. Artif. Intell.* **2022**, *118*, 105684. [CrossRef]
23. Wang, D.; Li, L. Fixed-time synchronization of delayed memristive neural networks with impulsive effects via novel fixed-time stability theorem. *Neural Netw.* **2023**, *163*, 75–85. [CrossRef] [PubMed]
24. Jia, T.; Chen, X.; Zhao, F.; Cao, J.; Qiu, J. Adaptive fixed-time synchronization of stochastic memristor-based neural networks with discontinuous activations and mixed delays. *J. Frankl. Inst.* **2022**, *360*, 3364–3388. [CrossRef]
25. Hu, C.; He, H.; Jiang, H. Fixed/Preassigned-time synchronization of complex networks via improving fixed-yime stability. *IEEE Trans. Cybern.* **2021**, *51*, 2882–2892. [CrossRef]
26. Rezaie, A.; Mobayen, S.; Ghaemi, M.; Fekih, A.; Zhilenkov, A. Design of a fixed-time stabilizer for uncertain chaotic systems subject to external disturbances. *Mathematics* **2023**, *15*, 3273. [CrossRef]
27. Yang, W.; Xiao, L.; Huang, J.; Yang, J. Fixed-time synchronization of neural networks based on quantized intermittent control for image protection. *Mathematics* **2021**, *23*, 3086. [CrossRef]
28. Pang, L.; Hu, C.; Yu, J.; Jiang, H. Fixed-time synchronization for fuzzy-based impulsive complex networks. *Mathematics* **2022**, *9*, 1533. [CrossRef]

29. Liu, H.; Cheng, J.; Cao, J.; Katib, I. Preassigned-time synchronization for complex-valued memristive neural networks with reaction-diffusion terms and Markov parameters. *Neural Netw.* **2023**, *169*, 520–531. [CrossRef] [PubMed]
30. Zhou, X.; Cao, J.; Wang, X. Predefined-time synchronization of coupled neural networks with switching parameters and disturbed by Brownian motion. *Neural Netw.* **2023**, *160*, 97–107. [CrossRef]
31. Yuan, J.; Zhang, C.; Chen, T. Command filtered adaptive neural network synchronization control of nonlinear stochastic systems with Lévy noise via event-triggered mechanism. *IEEE Access* **2021**, *9*, 146195–146202. [CrossRef]
32. Yao, W.; Wang, C.; Sun, Y.; Gong, S.; Lin, H. Event-triggered control for robust exponential synchronization of inertial memristive neural networks under parameter disturbance. *Neural Netw.* **2023**, *164*, 67–80. [CrossRef] [PubMed]
33. Bao, Y.; Zhang, Y.; Zhang, B. Fixed-time synchronization of coupled memristive neural networks via event-triggered control. *Appl. Math. Comput.* **2021**, *411*, 126542. [CrossRef]
34. Zhu, S.; Bao, H. Event-triggered synchronization of coupled memristive neural networks. *Appl. Math. Comput.* **2022**, *415*, 126715. [CrossRef]
35. Ge, C.; Liu, X.; Liu, Y.; Hua, C. Event-triggered exponential synchronization of the switched neural networks with frequent asynchronism. *IEEE Trans. Neural Netw. Learn. Syst.* **2024**, *35*, 1750–1760. [CrossRef] [PubMed]
36. Guo, H.; Liu, J.; Ahn, C.; Wu, Y.; Li, W. Dynamic event-triggered impulsive control for stochastic nonlinear systems with extension in complex networks. *IEEE Trans. Circuits Syst. I Regul. Pap.* **2022**, *69*, 2167–2178. [CrossRef]
37. Sun, J.; Wang, Y.; Wu, Y.; Zhou, Y.; Liu, J. Dynamic event-triggered control for fixed-time synchronization of Kuramoto-Oscillator networks with and without a pacemaker. *Intell. Control Appl.* **2023**, *111*, 10147–10162. [CrossRef]
38. Ge, C.; Chang, C.; Liu, Y.; Hua, C. Dynamic event-triggered exponential synchronization for neural networks with random controller gain perturbations. *Int. J. Control Autom. Syst.* **2023**, *21*, 2927–2937. [CrossRef]
39. Jia, S.; Hu, C.; Jiang, H. Fixed/Preassigned-time synchronization of fully quaternion-valued cohen–grossberg neural networks with generalized time delay. *Mathematics* **2023**, *11*, 4825. [CrossRef]
40. Li, R.; Cao, J. Dissipativity and synchronization control of quaternion-valued fuzzy memristive neural networks: Lexicographical order method. *Fuzzy Sets Syst.* **2021**, *443*, 70–89. [CrossRef]
41. Li, R.; Gao, X.; Cao, J. Quasi-state estimation and quasi-synchronization control of quaternion-valued fractional-order fuzzy memristive neural networks: Vector ordering approach. *Appl. Math. Comput.* **2019**, *362*, 124572. [CrossRef]
42. Li, R.; Cao, J.; Li, N. Quasi-synchronization control of quaternion-valued fuzzy memristive neural networks. *Fuzzy Sets Syst.* **2023**, *472*, 108701. [CrossRef]
43. Zhang, Z; Wang, S.; Wang, X.; Wang Z.; Lin, C. Event-triggered synchronization for delayed quaternion-valued inertial fuzzy neural networks via nonreduced order approach. *IEEE Trans. Fuzzy Syst.* **2023**, *31*, 3000–3014. [CrossRef]
44. Wei, R.; Cao, J. Synchronization control of quaternion-valued memristive neural networks with and without event-triggered scheme. *Cogn. Neurodyn.* **2019**, *13*, 489–502. [CrossRef] [PubMed]
45. Clarke, F. *Optimization and Nonsmooth Analysis*; Wiley: New York, NY, USA, 1983.
46. Filippov, A. *Differential Equations with Discontinuous Right-Hand Sides*; Kluwer: Boston, MA, USA, 1988.
47. Huang, L.; Guo, Z.; Wang, J. *Theory and Applications of Differential Equations with Discontinuous Right-Hand Sides*; Science Press: Beijing, China, 2011.
48. Aubin, J.; Frankowska, H. *Set-Valued Analysis*; Birkhäuser: Boston, MA, USA, 1990.
49. Wei, W.; Hu, C.; Yu, J.; Jiang, H. Fixed/preassigned-time synchronization of quaternion-valued neural networks involving delays and discontinuous activations: A direct approach. *Acta Math. Sci.* **2022**, *43*, 1439–1461. [CrossRef]